Technical Report
TR-16-09
February 2017

Microbial sulphide-producing activity in water saturated MX-80, Asha and Calcigel bentonite at wet densities from 1 500 to 2 000 kg m^{-3}

Andreas Bengtsson
Anders Blom
Björn Hallbeck
Carl Heed
Linda Johansson
Johanna Stahlén
Karsten Pedersen

SVENSK KÄRNBRÄNSLEHANTERING AB

SWEDISH NUCLEAR FUEL
AND WASTE MANAGEMENT CO

Box 250, SE-101 24 Stockholm
Phone +46 8 459 84 00
skb.se

SVENSK KÄRNBRÄNSLEHANTERING

ISSN 1404-0344
SKB TR-16-09
ID 1546731
February 2017

Microbial sulphide-producing activity in water saturated MX-80, Asha and Calcigel bentonite at wet densities from 1 500 to 2 000 kg m^{-3}

Andreas Bengtsson, Anders Blom, Björn Hallbeck, Carl Heed, Linda Johansson, Johanna Stahlén, Karsten Pedersen

Microbial Analytics Sweden AB

Keywords: KBP4000.

Abstract

The bentonite buffer that will surround copper canisters with spent nucelar fuel (SNF) in Sweden's future repository must maintain a high density to be able to sufficiently protect the canisters. Naturally occurring sulphate-reducing bacteria (SRB) in the bentonite and in surrounding groundwater may potentially threaten the integrity of the canisters by dissimilatory reduction of sulphate to sulphide, a substance corrosive to metals such as copper. Microbial sulphide-producing activity has been observed to decrease with increasing density but it is yet not known if there is a wet density above where microbial activity is impossible. Such a value may vary between different types of bentonite. In this report three different bentonite clays, Wyoming MX-80, Asha and Calcigel at wet densities ranging from 1 500 to 2 000 kg m^{-3} were investigated for microbial sulphide-producing activity as a function of bentonite wet density at full water saturation.

Test cells of titanium were used in the experiment which consisted of a cylinder with a piston inside. The cells were filled with bentonite clay powder with addition of a bacterial cocktail consisting of three different species of SRB, except controls without added SRB. By adjustment of the amount of bentonite in an invariable confined space, the swelling pressure generated by the bentonite could be regulated and also monitored by a force transducer connected to a data collection system. The bentonite clay powder was compacted to a specific volume and then water saturated with a salt solution through inlets at the bottom and top of the test cells. When the clay had reached the planned wet densities and was fully water saturated, the piston and bottom lids were removed. A 40 µm pore size titanium filter was attached to the bottom lid and kept the clay from swelling into the inlet hole. This filter was at start of the experiments replaced with a copper disc that simulated a copper canister. On the opposite clay core side to the copper disc, $^{35}SO_4^{2-}$ together with lactate were added. The test cells were then closed again and the force transducer, piston and top lid were refitted. The test cells were harvested in series after up to 123 days from the addition of $^{35}SO_4^{2-}$ and lactate. The radioactivity of the $Cu_x{}^{35}S$ that had formed on the copper discs was located and quantified using electronic autoradiography. Samples were taken from different layers of the bentonite core and analysed for distribution of ^{35}S, of sulphate and most probable number of SRB.

The results for the three clays indicated intervals from 1 740–1 880 kg m^{-3} in wet densities within which sulphide-producing activity as analysed by the copper discs dropped from high to very low or below detection. The studied commercial bentonites were all infested with cultivable SRB. While cultivability of SRB clearly decreased with increasing swelling pressure of MX-80 and Calcigel, it remained relatively constant for most tested wet densities applied to Asha. Maintaining a wet density above ~1 900 kg m^{-3} of bentonite buffers in future spent nuclear fuel repositories may consequently significantly reduce the risk for sulphide production in the buffer and concomitant corrosion of metal canisters.

Sammanfattning

Bentonitbufferten som kommer att omge kopparkapslar med uttjänt kärnbränsle i Sveriges framtida slutförvar måste upprätthålla en hög densitet för att kunna skydda kapslarna tillräckligt. Naturligt förekommande sulfatreducerande bakterier (SRB) i bentoniten och i omgivande grundvatten kan potentiellt hota kapslarnas livslängd genom katabolisk reduktion av sulfat till sulfid, ett ämne som är korrosivt för metaller såsom koppar. Mikrobiell sulfidproducerande aktivitet har observerats avta med ökande densitet men det är ännu inte känt om det finns ett tröskelvärde för våtdensitet där mikrobiell aktivitet helt avstannar. Ett sådant värde kan variera för olika typer av bentonitleror. I denna rapport undersöktes tre olika bentonitleror, Wyoming MX-80, Asha och Calcigel, vid våtdensiteter i ett intervall från 1 500 till 2 000 kg m^{-3}, för mikrobiell sulfidproducerande aktivitet som en funktion av våtdensitet vid full vattenmättnad.

I experimentet användes testceller av titan som bestod av en cylinder med en kolv inuti. Testcellerna fylldes med ett fintmalt pulver av bentonitlera med tillsats av en bakteriecocktail innehållande tre olika arter av SRB, förutom kontroller som var utan bakteriell tillsats. Genom att justera mängden bentonitlera i en sluten konstant volym kunde svälltrycket som genererades av bentoniten regleras och också mätas genom tryckceller som kopplats till ett datainsamlingssystem. Den finmalda bentonitleran kompakterades till en specifik volym och vattenmättades därefter med en saltlösning som flödades in genom inlopp i topp och botten på testcellen. När leran hade nått de planerade våtdensiteterna och var fullt vattenmättad togs kolven och bottenlocket bort. Ett titanfilter med en porstorlek på 40 µm var monterat på bottenlocket som förhindrade att leran svällde ut genom inloppshålet. Detta filter byttes i starten på experimentet ut mot en koppardisk som simulerade en kopparkapsel. På andra sidan av bentonitkärnan, motsatt koppardisken, tillsattes $^{35}SO_4^{2-}$ tillsammans med laktat. Testcellerna stängdes därefter igen och tryckcellen, kolven och topplocket återmonterades. Testcellerna analyserades sedan i serier upp till 123 dagar från tillsatsen av $^{35}SO_4^{2-}$ och laktat. Radioaktiveten från $Cu_x{}^{35}S$ som bildats på koppardiskarna lokaliserades och kvantifierades genom elektronisk autoradiografi. Prover togs från olika lager i bentonitkärnan och analyserades för distribution av ^{35}S, sulfat och odlingsbarhet (MPN) av SRB.

Resultaten för de tre lerorna indikerar att i ett intervall av våtdensitet från 1 740–1 880 kg m^{-3} går den sulfidproducerande aktiviteten, mätt på koppardiskarna, ner från hög till väldigt låg eller under den detekterbara gränsen. Alla de studerade kommersiella bentonitlerorna innehöll odlingsbara SRB. Medan odlingsbarheten helt klart minskade med ökande svälltryck för MX-80 och Calcigel så höll sig odlingsbarheten relativt konstant för de flesta undersökta densiteter för Asha. Att upprätthålla en våtdensitet över ~1 900 kg m^{-3} för bentonitbufferten i framtida slutförvar för kärnbränsle kan följaktligen signifikant minska risken för sulfidproduktion i bufferten och efterföljande korrosion av metallkapslar.

Contents

Abbreviations used in the report

Abbreviation	Meaning
SRB	Sulphate-reducing bacteria
DSMZ	German collection of microorganisms and cell cultures
AODC	Acridine orange direct count method
gdw	Gram dry weight
gww	Gram wet weight
AGW	Analytical grade water
MPN	Most probable number
LSC	Liquid scintillation counting
RedRate	Rate of sulphate to sulphide reduction
cpm	Counts per minute
dps	Disintegrations per second

1 Introduction

In the Finnish and Swedish repository concepts for geodisposal of spent nuclear fuel (SNF) the bentonite barrier has an important function in maintaining the integrity of the copper canisters isolating the SNF (SKB 2010). In the repository a highly compacted bentonite with a bulk wet density between 1 950 and 2 050 kg m^{-3} is projected. The bentonite is intended to hinder outward transport of radionuclides and inward transport of corrosive groundwater components, and to act as a buffer against rock movements. The presence and activity of sulphide-producing bacteria have been detected in groundwater at repository depth (Hallbeck and Pedersen 2012, Pedersen et al. 2014a) as well as in various types of commercially available bentonites including Asha, Calcigel and Wyoming MX-80 (Svensson et al. 2011). Sulphide-producing bacteria have been found in a full scale demonstration repository (Arlinger et al. 2013), in various pilot and full scale tests of bentonite performance (Karnland et al. 2009, Lydmark and Pedersen 2011) and in the Boom Clay formation (Bengtsson and Pedersen 2016). In a future SNF repository, the dominant long-term copper corrosive agent may, therefore, be sulphide. The anaerobic microbial process of concern is consequently the dissimilatory reduction of sulphate to hydrogen sulphide by sulphate-reducing bacteria (SRB).

One sulphate-reducing bacterium can produce $1–2 \times 10^{-15}$ mole sulphide from sulphate per hour (Hallbeck 2014, Jørgensen 1978). It has been shown that SRB in deep groundwater can keep up with this rate when provided with H_2 at concentrations not much higher than 1 μM (Pedersen 2012a, b). Analysis of numbers of SRB in commercial MX-80, Calcigel and Asha bentonites showed 56 000–130 000 cultivable SRB kg^{-1} $bentonite^{-1}$ during the alternative buffer material project at Äspö (Svensson et al. 2011). With 350 mm of bentonite surrounding the canister at a wet density of 2 000 kg m^{-3}, there will be approximately 50 SRB mm^{-2} of canister surface that have the potential to produce $10^2 \times 10^{-15}$ mole sulphide mm^{-2} h^{-1} which could cause problems for the sustainability of a SNF disposal canister in a long time span of 100 000 years or more. Although this number is conservative and comes with very large uncertainty, the number demonstrates that it does not take very many active SRB per kg of bentonite to challenge the integrity of the canister. If given good growth conditions, i.e. carbon and energy sources and sulphate, the SRB can rapidly multiply several orders of magnitude and then the produced sulphide over time may become far too large. Therefore, it is required to confirm the present hypothesis that sulphide-producing activity of SRB will be very slow or nil in the planned bentonite density range and concomitant swelling pressures. Microbial activity has been demonstrated to decrease with increasing density of bentonite (Motamedi et al. 1996, Motamedi 1999, Stroes-Gascoyne et al. 1997). Previous work with Wyoming MX-80 bentonite suggested that microbial sulphide-producing activity and cultivability cease somewhere in the range of 1 900–2 100 kg m^{-3} wet density, but the exact cut-off density remained to determine (Masurat et al. 2010, Pedersen et al. 2000a, b). Variables of importance for such activity, in addition to bentonite density can be swelling pressure, pore space and pore water composition, transport conditions to and from the bentonite boundaries, usability of the naturally occurring organic matter present in the bentonite and H_2 from corroding metals, H_2 and CH_4 from geological sources and temperature. The type of bentonite may also have a large influence on survival and activity of SRB.

Until now, laboratory research on survival and activity of SRB in bentonite as functions of density and swelling pressure has only been performed with Wyoming MX-80 bentonite at wet densities of 1 750 and 2 000 kg m^{-3} (Bengtsson et al. 2015). While the sulphide-producing activity was significant at 1 750 kg m^{-3} it was close to nil at 2 000 kg m^{-3}. A precise threshold could not be identified.

This work seeked to identify possible threshold bentonite wet densities for MX-80, Asha and Calcigel above which microbial sulphide-producing activity is practically inhibited, all others conditions being favourable for the microbes. This work also seeked to evaluate how viability of SRB decreases as wet density increase. Favourable conditions were obtained by the addition of lactate which is a preferred carbon and energy source for most SRB. Pure cultures of SRB were added to ensure that all experiments except controls included approximately an equal number of SRB plus possibly already present SRB in the commercial clays.

Cylindrical test cells made of titanium were used in the experiments. The cells were filled with the respective bentonite clay powder with addition of a bacterial cocktail consisting of three different species of SRB, except control cells that were filled with clay without added SRB. By adjustment of the amount of bentonite in an invariable corresponding space, the swelling pressure generated by the bentonite could be regulated and also monitored by force transducers connected to a data collection system. The bentonite clay powders were compacted to a specific volume and then water saturated with a salt solution. A copper disc that simulated a copper canister was installed in the clay core bottom when the clay cores had reached the planned wet densities and was fully water saturated. On the opposite clay core side to the copper disc, $^{35}SO_4^{2-}$ together with lactate, which is a preferred carbon and energy source for SRB, were added. This radioactive substance was used as a tracer for microbial reduction of sulphur in sulphate to sulphide. The test cells were then closed again and the force transducer, piston and top lid were refitted. The test cells were sampled in series after up to 123 days from the addition of $^{35}SO_4^{2-}$ and lactate. The radioactivity of $Cu_x{}^{35}S$ that had formed on the copper discs was located and quantified using electronic autoradiography. Samples were taken from different layers of the bentonite core and analysed for distribution of ^{35}S, of sulphate and most probable number of cultivable SRB. Sulphide production rates were calculated.

2 Material and method

2.1 Experiments

This report describes five different, consecutive experimental series with three different bentonite types and three different species of added SRB exposed to varying levels of wet density. To more easily refer to each experiment, a numbered list with information about bentonite types, planned densities and the time frame of the respective experiment 1 to 5 is given in Table 2-1. Experiment 1 with two densities of MX-80 was performed differently compared to experiments 2–5 in several aspects and these procedures and the obtained results have been reported (Bengtsson et al. 2015). The results from that report are included in this report for comparison with one additional MX-80 density in experiment 2 and with Asha and Calcigel. In experiment 1, negative controls were heat treated in an oven for one week at 110 °C in a partly unsuccessful attempt to sterilize the clay without altering the clay minerals. The copper discs were not bevelled in experiment 1 which resulted in a skewed distribution of results as previously described for Boom Clay experiments (Bengtsson and Pedersen 2016) and the number of clay sampling positions were different. Else, all procedures in experiment 1 was similar to the procedures in experiment 2–5.

Table 2-1. List of performed experiments with MX-80, Asha and Calcigel bentonites with the planned wet and dry densities.

Experiment number	Year	Bentonite(s) tested	Planned wet densities (kg m^{-3})	Planned dry densities (kg m^{-3})
1	2012–2013	MX-80	1750, 2000	1171, 1562
2	2013–2014	Asha,	1850, 1900, 1950, 2000	1300, 1406, 1453, 1529
		MX-80	1900	1406
3	2014–2015	Calcigel	1850, 1900, 1950	1333, 1411, 1490
4	2015–2016	Asha	1500, 1750, 1850	765, 1147, 1300
5	2016	Asha	1600, 1700	917, 1070

2.2 Chemical and mineralogical characters of the bentonites

The main mineralogical and chemical compositions of the clays are given in Table 2-2. All clays have a high content of montmorillonite and minor amounts of various clay minerals. MX-80 and Asha are sodium bentonites while Calcigel is a calcium bentonite as reflected by the respective amounts of CaO and Na_2O. The MX-80 contains more silica than Asha and Calcigel. Asha distinguishes form the other clays by a three times larger amount of iron and Calcigel distinguishes form the other clays by a smaller amount of montmorillonite and absence of sulphate. All clays contain carbon, possibly in carbonates, and organic carbon is present in MX-80 and Asha. Sulphur is found in all clays. The Asha used in this work was denoted Asha2012 (Sandén et al. 2014). All three clays were selected and delivered by SKB except for MX-80 in experiment 1 that was delivered from Clay Tech, Ideon, Lund, Sweden.

Table 2-2. Average results from the XRD analyses of mineral compositions and the composition of the MX-80 (n=6) (Karnland 2010), Asha (n=> 5) (Karnland 2010, Sandén et al. 2014) and Calcigel (n=2 (Herbert and Moog 2002) bentonite materials expressed as weight percent of major element oxides, total carbon and sulphur of dry mass after ignition. LOI denotes the percent mass loss due to ignition. n: number of independent samples; – = no data.

Component	MX-80	Asha	Calcigel
Minerals			
Montmorillonite	81	82	66
Muscovite	3.4	1.9	14
Plagioclase	3.5	0.82	3
Pyrite	0.6	0.66	0
Quartz	3.0	1.2	8.2
Other	8.5	13.4	8.8
Elements			
S-total	0.042	0.10	0.03
S-Sulphate	0.042	0.05	–
S-Sulphide	0.045	0.05	–
SiO_2	67.4	55.7	54.7
Al_2O_3	21.2	21.6	17.5
Fe_2O_3	4.14	14.8	5.05
MgO	2.61	2.16	3.37
CaO	1.46	0.87	2.94
Na_2O	2.25	2.32	0.47
K2O	0.55	0.14	1.16
TiO_2	0.17	2.19	0.41
P_2O_5	0.05	0.06	0.10
Total carbon	0.36	0.26	0.43
Organic carbon	0.24	0.22	< 0.02
LOI	9.9	15.4	–

2.3 Test cells

Identical test cells were used to create saturated bentonite cores in series with different densities. A test cell consisted of a titanium cylinder with top and bottom lid attached by six Allen screws for each lid. A piston operated inside the cylinder (Figure 2-1). When the piston was at its most extended position, a 35 × 20 mm confined cavity was produced inside the cylinder (Figure 2-2). This cavity was filled with MX-80, Asha or Calcigel bentonite powder (see Section 2.6). By using spacers (not shown) on the screws running through the top lid the volume inside the test cell was kept constant. The pressure created by the swelling bentonite pushed the piston upwards and by doing so a force transducer mounted between the piston and top lid was compressed. The amount of compression, which stood in direct correlation to the bentonite swelling pressure, was recorded by a data collection system connected to a computer (see Section 2.4). During the water saturation phase of each experiment (described in detail in Section 2.7) a water saturation (WS) bottom lid and piston were used. The lid had a 2 mm inlet hole which allowed water to enter the test cell and reach the bentonite. In addition, the piston had a longitudinal inside hole to get water inflow from both top and bottom. To stop the bentonite from swelling into the inlet holes, and also to get an evenly distributed inlet flow, a 40 μm pore size titanium filter was mounted with two Phillips screws on the inside of the saturation lid and piston. After the saturation phase the bottom lid and piston were replaced with a lid and a piston without inlet. The new piston was equipped with a removable ventilation plug to not trap gas inside of the test cell upon insertion of the piston. The titanium filter on the saturation bottom lid was replaced with a copper disc.

Figure 2-1. *View of all parts included in a test cell. All parts in contact with the bentonites were made of titanium. See text for details. WS = water saturation.*

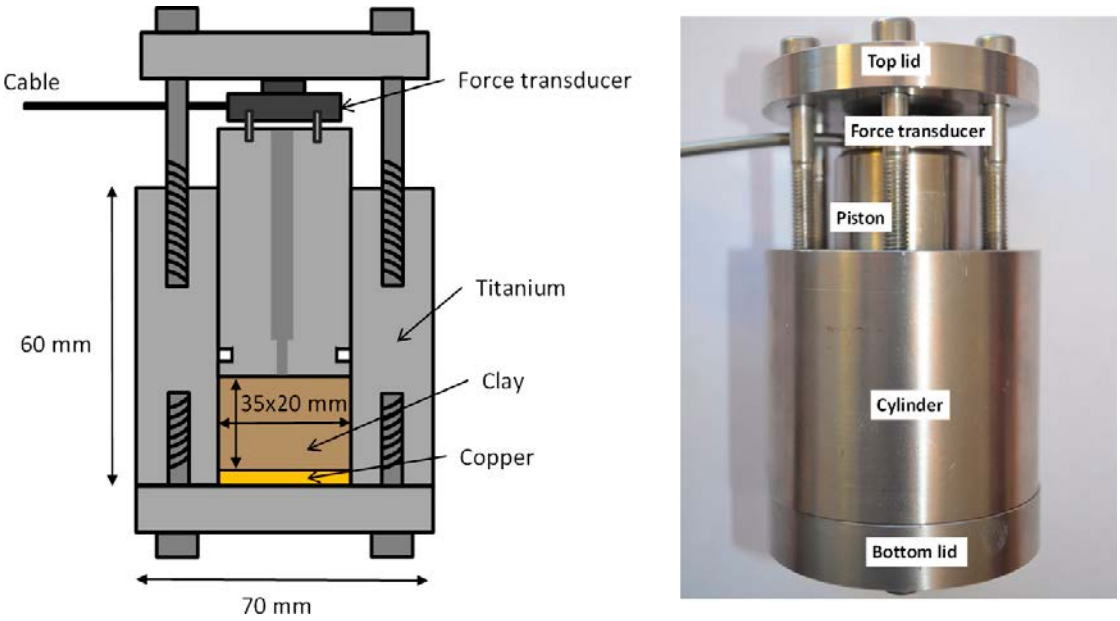

Figure 2-2. *Left: A schematic cross section of a test cell. Right: An assembled test cell, spacers are not mounted.*

2.4 Force transducer and data collection

The force transducers used to register the swelling pressure from the bentonite were purchased from Stig Wahlström Automatik, Stockholm, Sweden and had a load range from 0 to 907 kg (AL131DL, Honeywell model 53). The force transducers were connected to a data collection system consisting of transducer amplifiers for strain gage (Stig Wahlström Automatik, model DR7DC), a programmable logic controller (model Direct Logic 06) and a PC with a custom built software (CRS Reactor Engineering, Stenkullen, Sweden) for calibration and monitoring of the force transducer signals. The readings from the transducers were calibrated form 0 to 5 MPa against two externally calibrated manometers (S-11, 0–6 MPa, 4–20 mV G1⁄2; WIKA – AB Svenska IndustriInstrument, Göteborg, Sweden).

2.5 Bentonite slurries

Three different species of SRB were used in the experiment. *Desulfovibrio aespoeensis* (DSM 10631), *Desulfotomaculum nigrificans* (DSM 574) and *Desulfosporosinus orientis* (DSM 765). *D. aespoeensis* was isolated from deep groundwater (Motamedi and Pedersen 1998), *D. nigrificans* is a thermophilic, spore-forming sulphide-producing bacterium and *D. orientis* is spore-forming sulphide-producing bacterium with the ability to grow with H_2 as source of energy. The bacteria were grown in appropriate media and temperatures as specified by the German collection of microorganisms and cell cultures (DSMZ). At the start day of the experiments bacterial numbers for each of the three bacterial cultures were determined in 1 mL samples using the acridine orange direct count method as devised by Hobbie et al. (1977) and modified by Pedersen and Ekendahl (1990).

The three different bacterial cultures were mixed into one cocktail and poured or sprayed carefully out on a bed of bentonite powder in a large glass Petri dish for each of the bentonite types. This created small lumps of bentonite with cocktail. The whole content of the Petri dish was then passed through a mesh where the lumps were pulverised with sterile spoons. This created batches of bacteria doped bentonite with a bacterial content of approximately 1×10^7 SRB g^{-1}. All the work was performed inside of an anaerobic box with an atmosphere consisting of 97 % N_2 and 3 % H_2, $O_2 < 1$ ppm (COY Laboratory Products, Grass Lake, MI, USA).

2.6 Compaction of bentonite

The day before compaction of the bentonite the water content was determined on both non-doped and the SRB-doped bentonite batches by heating 3 × 1 g of each batch in aluminium bowls in 105 °C for 20 h. The average of the weight difference before and after heating for the three replicates was thus equal to the initial water content of each bentonite batch. The amount of bentonite (m_{solids}) needed to obtain the planned wet density for each test cell was calculated using the following equation (from Karnland 2010).

$$m_{solids} = V_{total} \times \rho_m - m_{max\ water}$$

Where ρ_m is the saturated density, m_{solids} is the mass of the solids, m_{max} water is the maximum possible mass of water, and V_{total} is the total volume of all components (solids and water). Grain densities were obtained from Karnland et al. (2006). The analysed dry and wet densities agreed with calculated values (± 1%).

Each test cell was assembled with bottom lid and a titanium filter and placed on an analytical scale where the calculated amounts of bentonite powder (m_{solids}), with or without added SRB, was weighed in. A water saturation piston was inserted in each test cell cylinder and in those cases where the bentonite powder volume was larger than the test cell volume (V_{total}) the bentonite powder was compacted with a workshop press (< 25 kg cm^{-2}) (Biltema, Göteborg, Sweden, cat no.15-846). Each test cell experiment was given a unique number and a code with information of the planned bentonite wet density, addition of SRB and incubation time: T or TC =test cell, 1 500–2 000 = 1 500 to 2 000 kg m^{-3} bentonite wet density, (+/−) = with or without adding of SRB, d=days of incubation. For test cell 1 in experiment 1 the code became: T1 1750 (−) 123d. Two different incubation times were used for

each experiment to be able to analyse microbial sulphide producing activity as a function of time. The incubation times i.e. time between start of the experiments and the sampling occasions varied slightly between different experiments but are still comparable.

In experiment 1 the bentonite and test cells were transported to Clay Technology AB in Lund, Sweden in air tight plastic containers so that the water content not would not be altered until compaction. The preparation and compaction was performed by Clay Technology personnel. For further information on this procedure, see Bengtsson et al. (2015).

2.7 Water saturation of bentonite

After compaction of the bentonite the test cells were assembled and mounted on a custom built water saturation system (Figure 2-3). A sterile salt solution was pushed into the evacuated (< 10 Pa) system with 200 kPa total pressure. The solution consisted of NaCl, 120 mM; $CaCl_2 \times 2H_2O$, 7 mM; KCl 9 mM; NH_4Cl, 18 mM; KH_2PO_4, 1 mM; $MgCl_2 \times 6H_2O$, 2 mM; analytical grade water (AGW) to 1 000 mL total volume. The solution was produced as described by Widdel and Bak (1992) for preparing anoxic media. The Calcigel clay does not contain leachable sulphate. Therefore, 1 mM of sodium sulphate was added to the solution to mimic a situation where natural sulphate-containing groundwater saturates the clay in a repository. MX-80 and Asha have large amounts of leachable sulphate.

Table 2-3. Saturation salt solution.

Addition	Amount
Analytical grade water (mL)	1 000
NaCl (g L^{-1})	7.0
$CaCl_2 \times 2H_2O$ (g L^{-1})	1.0
KCl (g L^{-1})	0.67
NH_4Cl (g L^{-1})	1.0
KH_2PO_4 (g L^{-1})	0.15
$MgCl_2 \times 6H_2O$ (g L^{-1})	0.5

Figure 2-3. *Water saturation system with twelve mounted test cells, receiving salt solution from both top and bottom. The pressure transmitting device is visible to the far right in the image.*

The pressures created by the swelling bentonites were monitored and the test cells were kept unaltered until stable swelling pressures presented themselves (see Appendix). Water could move freely in and out of the bentonite during the water saturation phase. In the second phase of the experiment where the two titanium filters were replaced with a copper disc and a 2 mm taller piston, respectively; water was not in contact with the clay. By using an identical confined space before and after contact with water, the swelling pressures were approximately reproduced as described next. In experiment 1 the pressures were regulated by forcing the pistons down on a weekly basis during the whole experimental time. In experiment 2 to 5, spacers used to set the confined volume inside of the test cells. They were kept fitted during the whole experimental time and the reproduced swelling pressures (RSPs) were not created by any mechanical extra load pressure. The final average RSPs registered by the force transducers correlated with the wet density at water saturation (Figure 2-4), confirmed at the end of the experiments.

2.8 Addition of $^{35}SO_4^{2-}$ and lactate

All work performed with additions of $^{35}SO_4^{2-}$ and lactate as well as the cleaning and insertion of the copper discs were carried out in the anaerobic box.

Copper discs were cleaned in an ultrasonic bath for 5 min in 99% ethanol and then rinsed with sterile analytical grade water (AGW) (Millipore Elix Essential 3, Millipore, Solna, Sweden). Afterwards the discs were placed in a beaker containing 250 mL gently stirred 0.5 M sulfamic acid (Aminosulfonic acid, H_2NSO_3H) (cat.nr. 24 277-2, Sigma-Aldrich) for 24 h, according to procedures for chemical cleaning of copper in ISO 8407:2010 – Corrosion of metals and alloys – Removal of corrosion products from corrosion test specimens (ISO 847:2009, IDT). The procedure was finished by sequentially washing the discs four times in glass beakers containing 400 mL sterilized, anoxic AGW at pH 7.

The test cells were disconnected from the water saturation system and the bottom lids with titanium filters, together with top lids and force transducers were removed. In each cell a copper disc with the same size as the titanium filter was inserted in the cavity that the filter left in the bentonite. A new bottom lid without inlet was attached to each test cell. The water saturation piston was carefully removed and batches of $Na_2{}^{35}SO_4$ (PerkinElmer, cat. no. NEX041H010MC, 10mCi (370MBq), specific activity: 1050–1600Ci (38.8–59.2 TBq $mmol^{-1}$ sodium sulphate in 1 mL water) distributed over the test cells by pipette to final calculated concentrations of 0.06, 0.06, 0.1, 0.07 or 0.06 µM in the pore water for experiments 1 to 5, respectively. The $Na_2{}^{35}SO_4$-solution was added to four equally spaced points on the bentonite core surface in each test cell (Figure 2-5). In addition, a 5.7 M lactate solution was added to a final calculated pore water lactate concentration of 28 mM in all test cells. The test cells were then reassembled with new pistons with ventilations plugs, force transducers and top lids. By once again attaching the spacers to the screws running through the top lids, the same inside confined volume as before isotope addition was obtained.

In experiment 1 (Bengtsson et al. 2015) and also in other experiments (Bengtsson and Pedersen 2016) a skewed distribution of microbial activity towards the edge of most, but not all copper discs were observed. This was most pronounced on the discs from test cells with high density bentonite. There was a very narrow, 2 mm deep space between the copper disc and the titanium wall of the test cells that was approximately 100 µm in width if the copper disc was perfectly centred. Any bentonite in this space followed the titanium filter when it was exchanged to a copper disc. It is possible that the space did not fill up with bentonite at full density. That would have opened up for microbial sulphate-reducing activity at a lower density and swelling pressure than planned in the space between the disc and the test cell wall and would explain most of the observed skewed distribution. In experiments 2–5 the titanium filters and copper disc edges were bevelled and the issue with skewed distribution was thereby mitigated.

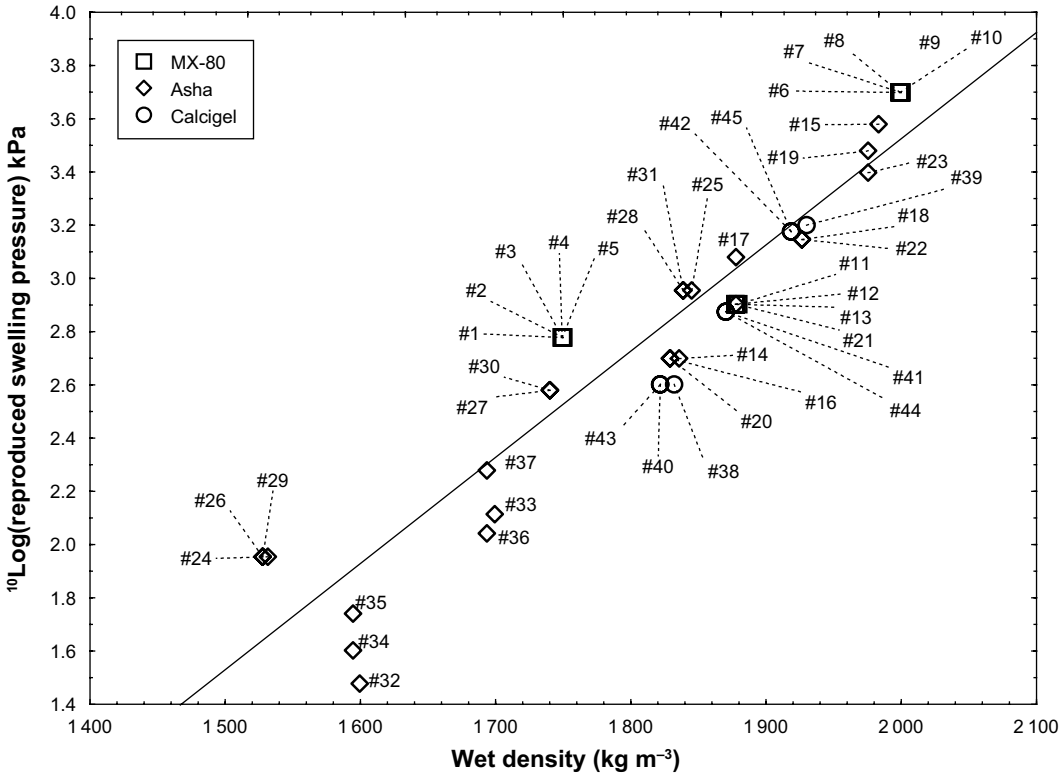

Figure 2-4. *Mean reproduced swelling pressures registered by the force transducers at full water saturation for the respective analysed wet density in all test cells in all experiments. The numbers refer to Table 2-5, Table 2-6 and Table 2-7 that show details on volumes, weight and water content for each test cell. The black line represents linear fit.*

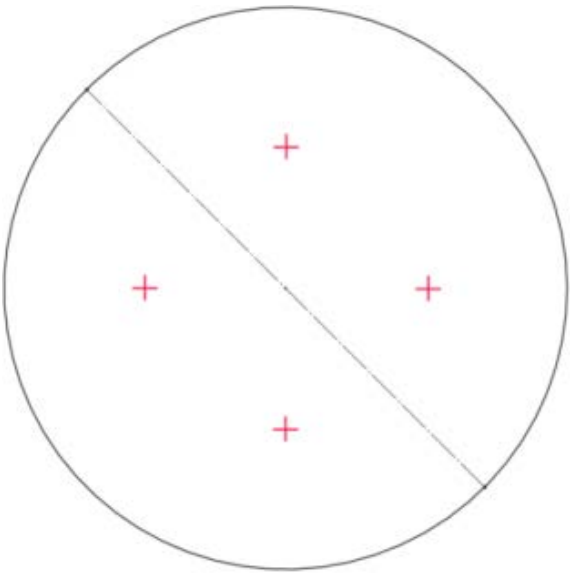

Figure 2-5. *Top view of a model test cell where + signs show the positions for addition of $^{35}SO_4^{2-}$ and lactate.*

2.9 Sampling and analysis

At the sampling date the pressure logging in the force transducer software was stopped, the force transducer was removed together with the top lid and screws. The top lid was then attached again, however with shorter screws to be able to push the piston all the way to the bottom. The test cells were moved to a fume hood and the bottom plates were carefully removed. The piston was then pressed up by turning the screws so that the edge of the copper disc became visible (Figure 2-6). An overview of analyses carried out on the copper discs and the bentonite cores is shown in Table 2-4.

Table 2-4. Overview of performed analyses for all test cells.

Analysis	Method
$Cu_x{}^{35}S$ on copper discs	2D surface autoradiography
Most probable number	Cultivation
Distribution of ^{35}S in bentonite cores	Liquid scintillation counting
Distribution of sulphate in bentonite cores	Turbidimetric method by precipitation of $BaSO_4$

2.9.1 Copper discs

The copper discs were removed with sterile tweezers and put in sterile Petri dishes and then immediately transferred to the anaerobic box where the Petri dishes were filled with anaerobic sterile AGW to completely cover the discs in order to remove bentonite residues and $^{35}SO_4{}^{2-}$. The discs were left in the Petri dishes for at least two hours.

After washing the discs were rinsed with sterile anaerobic AGW 5 times in separate beakers and then left to dry inside of the anaerobic box. When dried, the radioactivity of the $Cu_x{}^{35}S$ that had formed on the copper discs was located and quantified using a Packard Instant Imager electronic autoradiography system (Packard Instrument Company, Meriden, CT, USA) as follows. The copper discs were first placed on a foam sheet that was used to obtain a uniform plate level in the imager. The Instant Imager was calibrated according to the manufacturer's instructions using a ^{14}C calibration source provided by the manufacturer (Packard). The scanning time in the Instant Imager was set to 30 min. The Instant Imager sampled radioactivity in 0.5×0.5 mm pixels. Each pixel delivered a gross radioactivity count that was used for modelling and calculating the total amount of Cu_xS formed on the discs (Figure 2-7).

Figure 2-6. Sampling of test cell 8 (T8 2000 (+) 47d). Left: pushing the piston up by tightening screws. Right: copper disc completely pushed out of the test cell.

Table 2-5. Weight and volume parameters for the water saturated MX-80 bentonite in each test cell. (gdw = gram dry weight, %ww = percent wet weight).

Bentonite type	Exp. no.	Point no. in Fig 2-4	Test cell code	Test cell volume (cm^3)	Amount of bentonite (gdw)	Pore water volume (mL)	Water content (%ww)
MX-80	1	1	T1 1750 (−) 123d	19.23	22.52	11.13	33.07
MX-80	1	2	T2 1750 (−) 123d	19.23	22.52	11.13	33.07
MX-80	1	3	T3 1750 (+) 47d	19.23	22.50	11.13	33.10
MX-80	1	4	T4 1750 (+) 77d	19.23	22.50	11.13	33.10
MX-80	1	5	T5 1750 (+) 123d	19.23	22.50	11.13	33.10
MX-80	1	6	T6 2000 (−) 123d	19.23	30.03	8.43	21.91
MX-80	1	7	T7 2000 (−) 123d	19.23	30.03	8.43	21.91
MX-80	1	8	T8 2000 (+) 47d	19.23	30.01	8.44	21.95
MX-80	1	9	T9 2000 (+) 77d	19.23	30.01	8.44	21.95
MX-80	1	10	T10 2000 (+) 123d	19.23	30.01	8.44	21.95
MX-80	2	11	TC11 1900 (−) 84d.	19.54	26.84	10.28	27.70
MX-80	2	12	TC12 1900 (+) 35d.	19.54	26.78	10.35	27.88
MX-80	2	13	TC13 1900 (+) 84d.	19.54	26.78	10.35	27.88

Table 2-6. Weight and volume parameters for the water saturated Asha bentonite in each test cell. (gdw = gram dry weight, %ww = percent wet weight).

Bentonite type	Exp. no.	Point no. in Fig 2-4	Test cell code	Test cell volume (cm^3)	Amount of bentonite (gdw)	Pore water volume (mL)	Water content (%ww)
Asha	2	14	TC1 1850 (−) 84d.	19.54	24.97	11.17	30.91
Asha	2	15	TC2 2000 (−) 84d.	19.54	29.38	9.70	24.82
Asha	2	16	TC3 1850 (+) 35d.	19.54	24.77	11.38	31.47
Asha	2	17	TC4 1900 (+) 35d.	19.54	26.23	10.90	29.35
Asha	2	18	TC5 1950 (+) 35d.	19.54	27.69	10.42	27.34
Asha	2	19	TC6 2000 (+) 35d.	19.54	29.14	9.94	25.42
Asha	2	20	TC7 1850 (+) 84d.	19.54	24.77	11.38	31.47
Asha	2	21	TC8 1900 (+) 84d.	19.54	26.23	10.90	29.35
Asha	2	22	TC9 1950 (+) 84d.	19.54	27.69	10.42	27.34
Asha	2	23	TC10 2000 (+) 84d.	19.54	29.14	9.94	25.42
Asha	4	24	TC27 1500 (−) 88d.	18.27	14.85	12.55	45.80
Asha	4	25	TC28 1850 (−) 88d.	19.54	25.25	10.90	30.15
Asha	4	26	TC29 1500 (+) 43d.	18.27	14.74	12.66	46.20
Asha	4	27	TC30 1750 (+) 43d.	19.54	22.12	12.08	35.32
Asha	4	28	TC31 1850 (+) 43d.	19.54	25.06	11.08	30.66
Asha	4	29	TC32 1500 (+) 88d.	18.27	14.74	12.66	46.20
Asha	4	30	TC33 1750 (+) 88d.	19.54	22.12	12.08	35.32
Asha	4	31	TC34 1850 (+) 88d.	19.54	25.06	11.08	30.66
Asha	5	32	TC35 1600 (–) 78d.	19.54	17.91	13.35	42.70
Asha	5	33	TC36 1700 (–) 78d.	19.54	20.90	12.32	37.09
Asha	5	34	TC37 1600 (+) 33d.	19.54	17.76	13.50	43.18
Asha	5	35	TC38 1600 (+) 78d.	19.54	17.76	13.50	43.18
Asha	5	36	TC39 1700 (+) 33d.	19.54	20.72	12.49	37.61
Asha	5	37	TC40 1700 (+) 78d.	19.54	20.72	12.49	37.61

Table 2-7. Weight and volume parameters for the water saturated Calcigel bentonite in each test cell. (gdw = gram dry weight, % ww = percent wet weight).

Bentonite type	Exp. no.	Point no. in Fig 2-4	Test cell code	Test cell volume (cm^3)	Amount of bentonite (gdw)	Pore water volume (mL)	Water content (%ww)
Calcigel	3	38	TC14 1850 (−) 99d.	19.54	25.50	10.65	29.47
Calcigel	3	39	TC15 1950 (−) 99d.	19.54	28.50	9.61	25.21
Calcigel	3	40	TC16 1850 (+) 56d.	19.54	25.18	10.97	30.33
Calcigel	3	41	TC17 1900 (+) 56d.	19.54	26.66	10.46	28.18
Calcigel	3	42	TC18 1950 (+) 56d.	19.54	28.15	9.96	26.13
Calcigel	3	43	TC19 1850 (+) 99d.	19.54	25.18	10.97	30.33
Calcigel	3	44	TC20 1900 (+) 99d.	19.54	26.66	10.46	28.18
Calcigel	3	45	TC21 1950 (+) 99d.	19.54	28.15	9.96	26.13

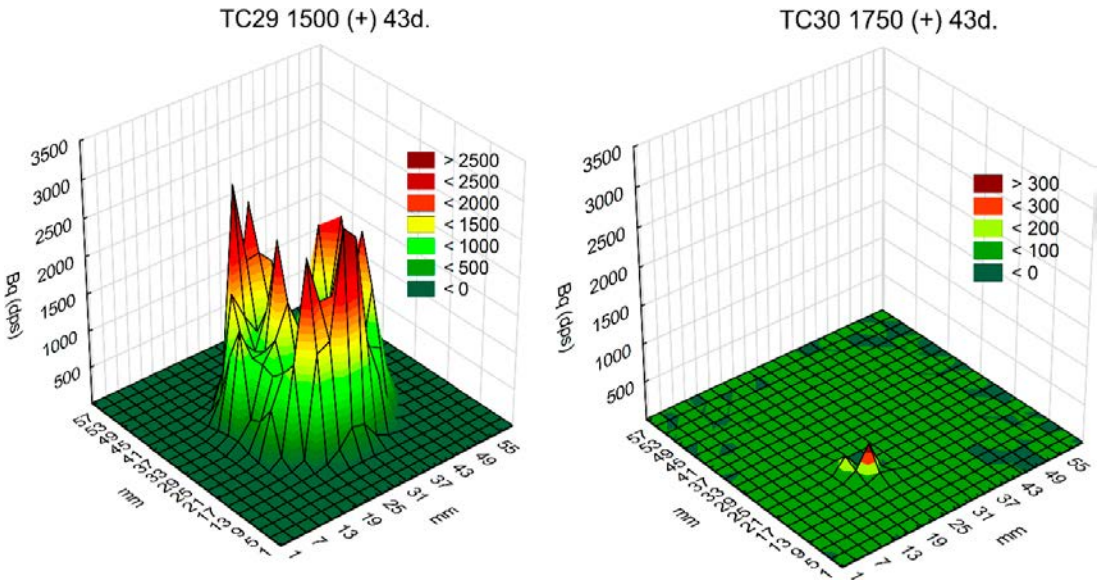

Figure 2-7. *3D plots showing emitted radiation per pixel in the autoradiography instrument for test cell 29 (left) and 30 (right) of experiment 4 with Asha bentonite after 43 days incubation. The plots illustrate a clear difference in emission, i.e. microbial sulphide-producing activity, between the two densities (1 500 kg m^{-3} and 1 750 kg m^{-3} wet density).*

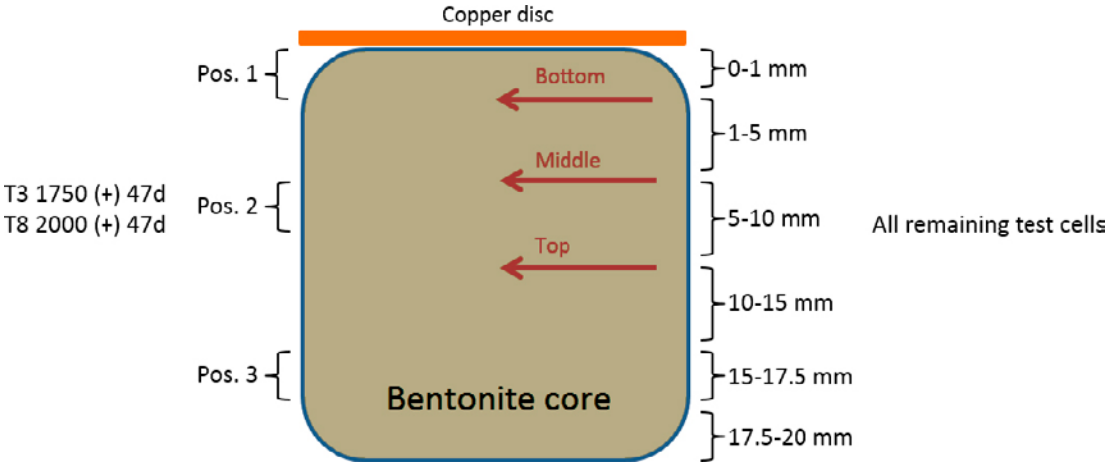

Figure 2-8. *Sampling positions and layers in bentonite cores. Left side describes sampling for test cell 3 and 8 in experiment 1. Right side describes sampling for all other test cells. Red arrows indicate sampling positions for MPN and water content samples referring to all test cells except 3 and 8 in experiment 1.*

2.9.2 Bentonite samples

In experiment 1, bentonite samples were taken out in three positions for test cell 3 and 8; close to the copper disc, in the middle of the bentonite core and close to the piston. The positions were denoted 1, 2 and 3 where number 1 was close to the copper surface and so on. Samples at each position were taken for analysis of most probable number (MPN) of SRB, water content and distribution of ^{35}S and sulphate in the bentonite (Figure 2-8).

For all other experiments the bentonite sampling method was modified in the following manner. Distribution of ^{35}S and sulphate were analysed from six different layers in the bentonite. The layers where: the first millimetre of bentonite closest to the copper surface (0–1 mm), the next four millimetres (1–5 mm), the next five millimetres (5–10 mm), the next five millimetres (10–15 mm), the next two and a half millimetres (15–17.5 mm) and the last two and a half millimetres (17.5–20 mm). One gram samples for MPN-analysis and water content analysis were taken on millimetre 1, 5 and 10 in the centre of the bentonite core (Figure 2-8).

2.9.3 Most probable number samples

Samples for MPN-analysis were transferred to the anaerobic box where tubes containing 1 gww (gram wet weight) of bentonite were filled with 20 mL sterile anaerobic 0.9 % NaCl solution and then put on shaker to disperse the bentonite. After the bentonite had dispersed (> 2 h) the samples were inoculated in five tubes for each of total two 10-time dilutions, resulting in an approximate 95% confidence interval lower limit of 1/3 of the obtained value and an upper limit of three times the value (Greenberg et al. 1992). The cultivation tubes were previousy filled with 9 mL anaerobic SRB growth medium, mixed as described by Widdel and Bak (1992) for preparing anoxic media and modified as described elsewhere (Pedersen et al. 2008). The MPN samples were cultured in 30 °C for four weeks before analysis. SRB were detected by measuring sulphide production using the $CuSO_4$ method according to Widdel and Bak (1992) on a UV visible spectrophotometer (Genesys UV 10, Thermo Electron Corporation).

2.9.4 Water content samples

Bentonite for water content analysis was carefully weighed in sterile, pre-weighed polypropylene tubes. The samples were then dried in a laboratory oven in 105 °C for 20 h and weighed again. The difference in weight before and after drying was taken as the bentonite water content (%ww in Table 2-5, Table 2-6 and Table 2-7). The calculated and analysed water contents differed at most 2%.

2.9.5 Distribution of ^{35}S in the bentonite core

Tubes containing bentonite samples for liquid scintillation counting (LSC) were kept in the fume hood after sampling and 40 mL of a sterile 10% $MgCl_2$ solution were added. The tubes were left for about a week to let the bentonite settle as a dispersed pellet in the bottom of the tubes. Afterwards, 100 µL of the supernatants were transferred to 24 mL scintillation vials (WHEA986581, VWR; Wheaton Industries, Stockholm, Sweden) containing 9.9 mL of a high-ionic scintillation cocktail (Biodegradable Counting Scintillant NBSC 104; Amersham Scientific). Counts per minute (cpm) for ^{35}S were measured in a Triathler LSC (Hidex, Turku, Finland), the counting time was 1 min. The scintillator's measuring efficiency was determined by analysing a 100 µL of $^{35}SO_4^{2-}$ (PerkinElmer, cat. no. NEX041H001MC, 1 mCi (37MBq), specific activity: 1050–1600Ci (38.8–59.2 TBq) $mmol^{-1}$, sodium sulphate in 1 mL water). The efficiency was 36 %.

2.9.6 Distribution of sulphate in the bentonite cores

From the same tubes as in Section 2.9.5 sulphate concentrations of the different positions or layers of the bentonite core were determined using the turbidimetric SulfaVer4 $BaSO_4$ precipitation method (Method #8051, range 2–70 mg L^{-1}, HACH Lange, Sköndal, Sweden), on undiluted or diluted samples. Dilution was performed in AGW to obtain optimal concentration range for analyses. Analyses were made on a HACH spectrophotometer model DR/2500 Odyssey (HACH Lange, Sköndal, Sweden). Sulphate analysis was also performed on raw bentonite before the start of each experiment to determine the amounts of lechable sulphate in each bentonite type. This was done by dispersing 1 g of bentonite

in 10, 20, 30, 40 and 50 mL of a 10% $MgCl_2$ solution. The concentration of sulphate was then measured with the SulfaVer4 method on diluted or undiluted supernatant from the five different tubes. To ensure that the entire sulphate was leached from the bentonite the remaining supernatant after analysis was poured off and the experiment was repeated with new $MgCl_2$ solution. Sulphate could not be detected in any of the tubes after the first leach.

2.10 Isotope calculations

Measured radioactivity counts were recalculated to mol ^{35}S in the form of $Cux_{35}S$ via Equation (2-1), based on a maximum Instant Imager detector efficiency of 2% (manufacturer's specification), as follows:

$$n = \left({}^{DPS}/_{\lambda} \Big/ N_A \right) \times 50 \qquad \text{Equation (2-1)}$$

where n is the number of mols, λ is the decay constant for ^{35}S, NA is Avogadro's constant and DPS is decays per second. The decay constant, λ, was calculated with Equation (2-2), as follows:

$$\lambda = \frac{\ln(2)}{t_{½}} \qquad \text{Equation (2-2)}$$

where $t_{1/2}$ is the half-life of ^{35}S (i.e., 7.55×10^6 s). Adjustment for decay of ^{35}S during the experimental time was made with Equation (2-3), as follows:

$$A = A_0 \times e^{-\lambda t} \qquad \text{Equation (2-3)}$$

where A is activity at time t, A_0 is activity at time zero and t is elapsed time. The amounts of $Cu_x{}^{35}S$ were then calculated using the total elapsed time between start of experiment and the measurement dates. The isotope dilution caused by nonradioactive, leachable sulphate in the pore water was calculated by dividing the analysed concentrations of sulphate by the concentration of radioactively labelled sulphate at the start of the experiments. The amount of $Cux^{35}S$ was multiplied by the isotope dilution factor to obtain the total amount of Cu_xS produced per copper disc. The amount of Cu_xS in mol on copper discs was calculated as follows: (Gross counts) / (count time in min) / 60 s/min / $\lambda/N_A \times 50 \times$ (isotope dilution factor). The factor of 50 is attributed to the Instant Imager's count efficiency of 2%, as specified by the manufacturer.

2.11 Determining the rate of microbial reduction of sulphate to sulphide

These calculations were adopted from publications by Pedersen (2010) and Bengtsson and Pedersen (2016). At start of the experiment the following was assumed to be known: The geometry of the clay core, the original amount of $^{35}SO_4{}^{2-}$ added and where it was deposited, the rate of decay of ^{35}S, and that the added SRB was evenly spread throughout the clays during the experiment. A good approximation of the diffusion coefficients for sulphate (2.0×10^{-12} m^2 s^{-1}) and sulphide (4.0×10^{-12} m^2 s^{-1}) in bentonite were adopted as discussed by Bengtsson et al. (2015). The amount of sulphide that reaches the copper discs at any given time was determined by computer simulations of changing conditions in the test cells. A mathematical model and a computer program were used to perform such simulations. By running this program with different assumed values on the sulphate reduction rate (RedRate) and comparing the resulting amounts of $Cu_x{}^{35}S$ on the copper disc in a mathematical model with the actual amounts found in the experiment test cells it was possible to determine values for RedRate for each test cell.

2.11.1 Mathematical model of test cells

The interior of the test cells was divided into a matrix of 31 cells in each direction. This means that $31 \times 31 \times 31 = 29\,791$ matrix cells were used to model a test cell where some matrix cells represented the test cell walls and the copper disc. The majority of the matrix cells represented the respective clay. Each cell held a specific amount of $^{35}SO_4^{2-}$ and $^{35}S^{2-}$. Each matrix cell also contained SRB that reduced sulphate to sulphide at a rate of RedRate per volume and time. Sulphate and sulphide were not allowed to diffuse through the test cell walls or the copper disc in the model and the initial amounts of $^{35}SO_4^{2-}$ and $^{35}S^{2-}$ were set to 0 in all matrix cells except four. These four matrix cells were positioned on the top surface of the clays in positions where $^{35}SO_4^{2-}$ was added (Figure 2-5).

2.11.2 Simulation program

The computer program utilized the finite difference method (Morton and Mayers 2005). The test cell volume was divided into small parts (matrix cells) and the changes in sulphate and sulphide concentrations in each matrix cell were repeatedly computed during short time intervals (dT). An explicit time integration scheme was used that is known to be stable and to converge if the criterion: $dT < 0.5 \times (\text{cell thickness})^2 / D_s$ is satisfied (Morton and Mayers 2005). In this convergence criterion D_s denotes the higher of the diffusion coefficients of sulphate and sulphide. The computer program was written in the programming language Visual Basic 6 running under Windows Vista on a regular PC. The change in sulphate concentration in each matrix cell during a time step (dT) was computed by adding the diffusion in/out of its adjacent matrix cells and subtracting the amount of sulphate converted to sulphide during the dT. The diffusion between matrix cells during a dT was computed with Fick's law (Coulson and Richardson 1990, 446–447). One way of writing Fick's law is Equation (2-4) below. The amount of sulphate reduced to sulphide during a dT (dSO_4red) was computed with Equation (2-5) below.

$$m' = \Delta C \times D \times A/d \text{ (Fick's law)} \quad (2\text{-}4)$$

m' = mass transport (mol s^{-1})

ΔC = concentration difference between cells (mol m^{-3})

D = Diffusions coefficient (m^2 s^{-1})

A = Surface area of boundary between two adjacent cells (m^2)

d = Distance between cell centres (m)

$$dSO_4red = \text{RedRate} \times \text{cell volume} \times dT \quad (2\text{-}5)$$

dSO_4red = amount of sulphate reduced to sulphide during a dT (mol)

RedRate = Rate of sulphate reduction to sulphide (mol m^{-3} s^{-1})

Cell volume (m^3)

dT (s)

2.12 Data processing, graphics and statistics

Data processing, statistical analyses and data visualizations were performed using Microsoft Office Excel 2016 (Microsoft Corporation, Redmond, USA) and Statsoft Statistica v 13 (Statsoft, Tulsa, USA) software.

3 Results

3.1 Bentonites

3.1.1 MX-80

The 1 750 kg m^{-3} and the 2 000 kg m^{-3} results were reported previously, and are included in this report for comparison with the results from 1 900 kg m^{-3} test cells. Immediately when the test cells were opened an obvious difference between the 1 750 kg m^{-3}, 1 900 kg m^{-3} and the 2 000 kg m^{-3} copper discs was observed. All the 1 750 kg m^{-3} discs had black precipitates of iron sulphide on the surface while the 1 900 and 2 000 kg m^{-3} discs were free from precipitates. When analysed in the Instant Imager autoradiograph, on average, a 10 000 times higher surface radioactivity was measured on the (+) 1 750 kg m^{-3} discs compared to the (+) 2 000 and (+) 1 900 kg m^{-3} discs (Table 3-1). Heat treatment of the bentonite did not have any significant sterilization effect in the (−) 1 750 kg m^{-3} cells that showed similar levels of radioactivity on the discs compared to the discs in (+) 1 750 kg m^{-3} cells with added SRB. This suggests that inherent SRB in the commercial bentonite survived heat treatment and were activated by the water addition to the bentonite.

In the 2 000 kg m^{-3} case the cells with added SRB showed a low level of sulphide-producing activity and the heat treated betonite did not show any radioactivity on their discs above the detection limit which is very low. The cells with added microbes showed small spots of $Cu_x{}^{35}S$ mostly on the edges of the discs. These spots were probably formed by germinating spore forming SRB that took advantage of heterogeneities in the bentonite or roughness of the copper discs. Furthermore, bentonite in the narrow boundary space between the test cell inner wall and the edge of the copper disc might not have reached up to full swelling pressure. This could explain why Cu_xS mostly was formed on the edges of these discs. In the centre were the wet density reached 2 000 kg m^{-3} only a few small radioactive spots were found. This demonstrates how extremely important the swelling pressure is for bacterial sulphide-producing activity in compacted bentonites.

Table 3-1. MX-80 reproduced swelling pressures deduced from data obtained with force transducers for each test cell, radioactivity detected on the copper discs recalculated for half-life of the isotope and the total amount of copper sulphide on the discs calculated from the surface activity and the isotope dilutions ($[SO_4^{2-}]/[^{35}SO_4^{2-}]$).

Test cell code	Mean reproduced swelling pressure (kPa)	Surface activity (kBq)	Total amount of Cu_xS (nmole)
MX-80			
T3 1750 (+) 47d.	600	1600	21600
T4 1750 (+) 77d.	600	1600	21400
T5 1750 (+) 123d.	600	528	7130
T1 1750 (−) 123d.	600	593	7630
T2 1750 (−) 123d.	600	1130	14500
TC12 1900 (+) 35d.	1000	0.05	1.17
TC13 1900 (+) 84d.	800	0.04	1.07
TC11 1900 (−) 84d.	800	0.03	0.675
T8 2000 (+) 47d.	5000	0.2	3.99
T9 2000 (+) 77d.	5000	0.1	1.47
T10 2000 (+) 123d.	5000	0.6	13.7
T6 2000 (−) 123d.	5000	0.0001	0.002
T7 2000 (−) 123d.	5000	0.0001	0.002

3.1.2 Asha

In the experiments described below copper discs with bevelled edges were used which eliminated the density issue with the bentonite in the narrow boundary space between the test cell inner wall the edge of the copper disc. With bevelled edged, the bentonite could swell properly around the edges of the titanium filters. Table 3-2 shows data from three different experiments performed at three different date intevals, however with the same experimental setup. The tested wet densities for the first experiment with Asha ranged from 1 850 to 2 000 kg m^{-3}. However, no substatial surface radioactivity was found on any of the copper discs in that experiment. Therefore, two new experiments with densities that ranged from 1 500 to 1 850 kg m^{-3} was performed. When evaluating all experiments together, a considerable surface radioactivity was found on the 1 500 to 1 700 kg m^{-3} discs but in all other densities the measured radioactivity on the discs were close to or at the detection limit (Table 3-2). In comparison with MX-80 (Table 3-1) where a high surface radioactivity was observed on discs incubated with 1 750 kg m^{-3} bentonite, low surface radioactivity was observed at the same wet density for Asha bentonite. There seems to be an additional factor that can limit the microbial activity in Asha bentonite compared to MX-80.

Table 3-2. Asha reproduced swelling pressures deduced from data obtained with force transducers, radioactivity detected on the copper discs recalculated for half-life of the isotope and the total amount of copper sulphide on the discs calculated from the surface activity and the isotope dilutions ($[SO_4^{2-}]/[^{35}SO_4^{2-}]$).

Test cell code	Mean reproduced swelling pressure (kPa)	Surface activity (kBq)	Total amount of Cu_xS (nmole)
Asha			
TC29 1500 (+) 43d.	90	1 070	12 000
TC32 1500 (+) 88d.	90	1 340	15 200
TC27 1500 (−) 88d.	90	311	3 380
TC37 1600 (+) 33d.	40	309	4 590
TC38 1600 (+) 78d.	55	736	10 900
TC35 1600 (–) 78d.	30	866	13 100
TC39 1700 (+) 33d.	110	807	13 200
TC40 1700 (+) 78d.	190	4	62.0
TC36 1700 (–) 78d.	130	0.99	16.4
TC30 1750 (+) 43d.	380	11.0	254
TC33 1750 (+) 88d.	380	191	4 450
TC3 1850 (+) 35d.	500	0.001	0.028
TC31 1850 (+) 43d.	900	0.01	0.162
TC7 1850 (+) 84d.	500	0.09	3.10
TC1 1850 (−) 84d.	500	0.001	0.021
TC34 1850 (+) 88d.	900	0.2	4.69
TC28 1850 (−) 88d.	900	0.03	0.774
TC4 1900 (+) 35d.	1 200	0.01	0.191
TC8 1900 (+) 84d.	800	0.01	0.413
TC5 1950 (+) 35d.	1 400	0.03	1.42
TC9 1950 (+) 84d.	1 400	0.0003	0.015
TC6 2000 (+) 35d.	3 000	0.002	0.106
TC10 2000 (+) 84d.	2 500	0.02	0.794
TC2 2000 (−) 84d.	3 800	0.0001	0.002

3.1.3 Calcigel

A clear difference in measured surface radioactivity between 1 850 and 1 900 kg m^{-3} was found in the Calcigel experiment (Table 3-3). The 1 850 kg m^{-3} case in Calcigel was the heaviest density were considerable microbial sulphide-producing activity could be analysed for the three tested bentonite types. The Calcigel bentonite had a very low natural sulphate content but still harboured inherent SRB in numbers well above the detection limit (Svensson et al. 2011). In the Calcigel experiment we added 1 mM sulphate to the saturation salt solution which evidently was enough to activate SRB present in this commercial bentonite since also the control test cell (TC14 1850 (−) 99d.) without any addition of SRB produced analysable amounts of radioactive $^{35}S^{2-}$ on the copper disc. However, it is not clear if the natural population of SRB would be activated at 1 850 kg m^{-3} without sulphate addition; this question requires further investigations.

Table 3-3. Calcigel reproduced swelling pressures deduced from data obtained with force transducers, radioactivity detected on the copper discs recalculated for half-life of the isotope and the total amount of copper sulphide on the discs calculated from the surface activity and the isotope dilutions ($[SO_4^{2-}]/[^{35}SO_4^{2-}]$).

Test cell code	Mean reproduced swelling pressure (kPa)	Surface activity (kBq)	Total amount of Cu_xS (nmole)
Calcigel			
TC16 1850 (+) 56d.	400	1 110	332
TC19 1850 (+) 99d.	400	1 580	484
TC14 1850 (−) 99d.	400	123	31
TC17 1900 (+) 56d.	750	9	3
TC20 1900 (+) 99d.	750	23	8
TC18 1950 (+) 56d.	1 500	43	16
TC21 1950 (+) 99d.	1 500	12	4
TC15 1950 (−) 99d.	1 600	0.03	0.01

3.2 MPN-samples

The MPN results demonstrate how well the SRB community survived in the three different bentonites during incubation. In contrast to the accumulated ^{35}S measurements on copper discs viable SRB could be cultivated from all tested densities (Figure 3-1). However, in wet densities higher than 1 850 kg m^{-3} only SRB from test cells with addition of SRB (one exception for Asha and one for MX-80) could be cultivated. This may indicate that the inherent, cultivable SRB populations in the tested bentonites were killed during the experiment in wet densities over 1 850 kg m^{-3}. Two of the added bacterial species (*D. orientis and D. nigrificans*) are able to form spores when introduced to an unsuitable environment. Spores are very tough and are able to withstand extreme conditions such as high pressures, high temperatures and drought. If the inherent populations lack spore-forming bacteria, that could explain the difference between viable and non-viable bacteria after an incubation in bentonite with a dry density over 1 850 kg m^{-3} (swelling pressure over 3 800 kPa). Alternatively, SRB may lose cultivability when stressed at high wet densities.

3.2.1 MX-80

Results from MPN analysis match the results from surface radioactivity measurement on the copper discs to some extent. In the 1 750 kg m^{-3} cases (added microbes or not) an increasing trend over time was found, with relatively high bacterial numbers from the latest sampling at 123 days compared to day 47 (Table 3-4). For the 2 000 kg m^{-3} case, low numbers of cultivable SRB were found in the test cells with added microbes and the numbers were below detection in the heat treated bentonite cells without addition of microbes, consistent with the surface radioactivity measurement on the copper discs from these test cells. Overall the viable SRB seemed to be evenly distributed through the bentonite core since similar numbers were found in all three positions for each test cell, except for some of the 1 750 kg m^{-3} cells where higher numbers were found in the top and bottom position compared to the middle (Table 3-4).

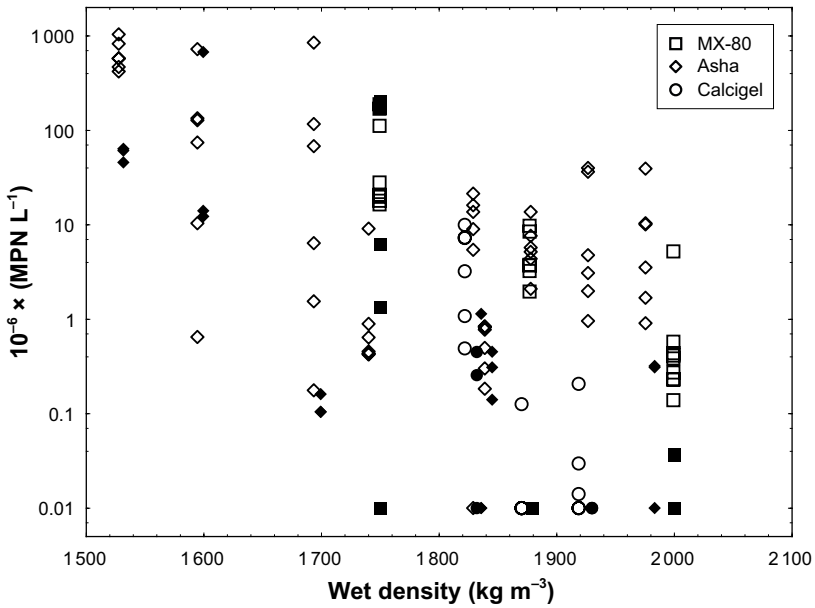

Figure 3-1. Most probable numbers of sulphate reducing bacteria in pore water of bentonite cores for three clays over wet density. Filled markers indicate control bentonite samples without bacterial addition. Values at 0.01 were below the detection limit of the MPN method.

Table 3-4. Most probable numbers of SRB in pore water of MX-80 the bentonite cores. Sample positions are shown in Figure 2-8.

	Position					
	Bottom (1 mm from copper discs)		Middle (5 mm from copper discs)		Top (10 mm from copper discs)	
Test cell code	10^{-6} × (MPN L^{-1})	Lower–upper 95% confidence interval	10^{-6} × (MPN L^{-1})	Lower–upper 95% confidence interval	10^{-6} × (MPN L^{-1})	Lower–upper 95% confidence interval
T3 1750 (+) 47d.	> 20	–	> 21	–	> 20	–
T4 1750 (+) 77d.	28	13–74	16	6–49	18	8–46
T5 1750 (+) 123d.	> 189	–	112	37–360	170	64–563
T1 1750 (−) 123d.	> 201	–	< 0.2	–	1	0.5–3
T2 1750 (−) 123d.	> 201	–	6	2–21	170	64–563
TC12 1900 (+) 35d.	3	1–11	2	1–8	4	1–10
TC13 1900 (+) 84d.	4	2–13	8	3–23	10	4–29
TC11 1900 (−) 84d.	< 0.1	–	< 0.1	–	< 0.1	–
T8 2000 (+) 47d.	0.6	0.2–1	0.4	0.2–1	5	2–13
T9 2000 (+) 77d.	0.4	0.2–1	0.1	0.04–0.4	0.3	0.1–0.7
T10 2000 (+) 123d.	0.2	0.1–0.6	0.4	0.2–1	0.2	0.1–0.6
T6 2000 (−) 123d.	< 0.04	–	< 0.04	–	< 0.04	–

3.2.2 Asha

Cultivable SRB were found in bentonite from every test cell in the Asha experiments, however with a significant positive bias towards the 1 500–1 700 kg m^{-3} wet density test cells (Table 3-5). As for MX-80 the cultivable SRB in Asha were also evenly distributed throughout the bentonite core sampling positions. On average the 1 900, 1 950 and 2 000 kg m^{-3} test cells with bacterial addition (+) had more viable SRB than had the 1 850 kg m^{-3} test cells. The expected result would be a decreasing trend of viable SRB with increasing bentonite density or a complete cut off after a certain density, similar to the results for accumulation of ^{35}S on the copper discs. Why this viability was observed for Asha test cells that did not show any microbial sulphide-producing activity when analysed for accumulation of ^{35}S on copper discs is at present unknown. It is obvious that bacteria survived well at all tested densities with no decreasing trend in viability with increasing density as was observed for MX-80 and Calcigel (Figure 3-1).

Table 3-5. Most probable numbers of SRB in pore water of the Asha bentonite cores. Sample positions are shown in Figure 2-8.

	Position					
	Bottom (1 mm from copper discs)		Middle (5 mm from copper discs)		Top (10 mm from copper discs)	
Test cell code	10^{-6} × (MPN L^{-1})	Lower–upper 95% confidence interval	10^{-6} × (MPN L^{-1}	Lower–upper 95% confidence interval	10^{-6} × (MPN L^{-1})	Lower–upper 95% confidence interval
TC29 1500 (+) 43d.	> 578	–	824	374–2 172	1 036	345–4 490
TC32 1500 (+) 88d.	> 577	–	> 420	–	470	176–1 557
TC27 1500 (−) 88d.	> 61	–	64	24–211	> 46	–
TC37 1600 (+) 33d.	74	28–246	128	59–300	0.6	0.3–1.8
TC38 1600 (+) 78d.	134	45–581	> 722	–	10	4–39
TC35 1600 (–) 78d.	677	254–2 242	12	4–49	14	5–56
TC39 1700 (+) 33d.	117	53–307	2	1–7	0.2	0.1–0.4
TC40 1700 (+) 78d.	68	29–175	6	2–19	846	317–2 801
TC36 1700 (–) 78d.	0.1	0.04–0.3	0.2	0.1–0.6	0.1	0.04–0.3
TC30 1750 (+) 43d.	0.4	0.2–1	1	0.2–2	0.5	0.2–1
TC33 1750 (+) 88d.	9	4–26	1	0.4–2	0.4	0.2–1
TC3 1850 (+) 35d.	14	5–51	21	9–73	5	2–15
TC31 1850 (+) 43d.	0.3	0.1–1	1	0.3–2	1	0.4–2
TC7 1850 (+) 84d.	< 1	–	16	5–64	9	4–24
TC1 1850 (−) 84d.	< 1	–	1	1–6	< 1	–
TC34 1850 (+) 88d.	1	0.4–2	0.5	0.2–2	0.2	0.1–1
TC28 1850 (−) 88d.	0.1	0.1–0.5	0.3	0.1–1	0.5	0.2–1
TC4 1900 (+) 35d.	2	1–8	5	2–16	4	2–14
TC8 1900 (+) 84d.	8	3–21	6	2–18	14	6–36
TC5 1950 (+) 35d.	1	0.4–3	3	1–10	5	2–15
TC9 1950 (+) 84d.	2	1–8	36	15–146	40	16–160
TC6 2000 (+) 35d.	2	1–7	> 10	–	10	4–34
TC10 2000 (+) 84d.	1	0.3–2	39	16–157	4	1–12
TC2 2000 (−) 84d.	0.3	0.1–1	0.3	0.1–1	< 1	–

3.2.3 Calcigel

For the test cells with bentonite at 1 850 kg m^{-3} wet density that had high numbers of accumulated ^{35}S on the copper discs (Table 3-3), lower numbers of cultivable SRB was found compared to test cells from MX-80 and Asha. This might be due to that Calcigel contains smaller numbers of natural bacteria in the raw bentonite material than the other two bentonites. In addition, the lowest tested density for Calcigel was 1 850 kg m^{-3} which was heavier than the lowest tested densities for Asha and MX-80. The viable SRB numbers probably would be higher if the Calcigel density was lowered to 1 500 or 1 750 kg m^{-3} where high bacterial numbers was observed for Asha and MX-80, respectively.

For the bottom and middle positions of test cell 16 and 19 it also appears that bacterial numbers decreased over time. However, when comparing with the measured surface activity, an opposite trend was observed where test cell 19 had more than double the accumulated ^{35}S on the copper disc than had test cell 16.

Table 3-6. Most probable numbers of SRB in pore water of the Calcigel bentonite cores. Sample positions are shown in Figure 2-8.

	Position					
	Bottom (1 mm from copper discs)		Middle (5 mm from copper discs)		Top (10 mm from copper discs)	
Test cell code	10^{-6} × (MPN L^{-1})	Lower–upper 95% confidence interval	10^{-6} × (MPN L^{-1})	Lower–upper 95% confidence interval	10^{-6} × (MPN L^{-1})	Lower–upper 95% confidence interval
TC16 1850 (+) 56d.	7	3–20	10	4–28	3	1–11
TC19 1850 (+) 99d.	0.5	0.2–1	1	0.4–3	7	3–22
TC14 1850 (−) 99d.	< 0.1	–	0.5	0.1–1	0.3	0.1–1
TC17 1900 (+) 56d.	< 0.1	–	< 0.1	–	< 0.1	–
TC20 1900 (+) 99d.	< 0.1	–	< 0.1	–	0.1	0.1–0.7
TC18 1950 (+) 56d.	0.2	0.1–1	< 0.01	–	0.01	0.01–0.07
TC21 1950 (+) 99d.	0.03	0.01–0.1	< 0.02	–	< 0.02	–
TC15 1950 (−) 99d.	< 0.02	–	< 0.02	–	< 0.02	–

3.3 Distribution of ^{35}S in the bentonite cores

In Figure 3-2 to Figure 3-4 the distributions of added ^{35}S in the bentonite cores are shown as nanomoles per litre pore water. Results were adjusted for the half-life of the ^{35}S isotope and the scintillation instrument efficiency (36 %). The analysis method does not separate $^{35}SO_4^{2-}$ from $H^{35}S^-$ in the bentonite pore water. The results show that the isotope had an evenly distribution through the bentonite cores with some exceptions in the analysed 1 and 2.5 mm layers close or remote to the copper discs.

The test cells containing bentonite with the largest volume of pore water, i.e. the test cells with lowest density, had a slightly lower concentration of ^{35}S after the experiment. The effect was most pronounced for MX-80 and Calcigel (Figure 3-2 and Figure 3-4 respectively). This would be expected if all test cells had been given an equal amount of radioactive isotope at the start of the experiment. Yet, the difference in pore water content was anticipated and accounted for when adding the isotope. However, in retrospect, the estimations of water content done before the experiments started were too low and in reality all test cells contained more water than calculated during planning, due to varying initial water contents of the bentonites. This means that the difference between calculated isotope concentrations and actual concentrations became more pronounced with rising bentonite density which would explain that the ^{35}S distribution and amount vary with density.

3.3.1 MX-80

In MX-80 the first and the last layer of the bentonite cores from experiment 1 (1 750 and 2 000 kg m^{-3}) had a higher concentration of ^{35}S than the rest of the bentonite core (Figure 3-2). In the remaining positions for all other MX-80 bentonite cores an even distribution of ^{35}S was observed.

3.3.2 Asha

An even distribution of ^{35}S was found in the Asha bentonite cores (Figure 3-3). Test cell 32 which had the highest value for accumulated $Cu_x{}^{35}S$ on its copper disc (Table 3-2) also had the lowest concentration of ^{35}S left in bentonite core after the experiment. Else, no correlation between density, microbial activity and distribution of ^{35}S could be observed.

3.3.3 Calcigel

The Calcigel bentonite cores had an even distribution of ^{35}S. However, the separation in ^{35}S concentration between test cells that contained bentonite with the same density was the largest in this experiment. Why test cell 15 had twice as high ^{35}S concentration than test cell 18 is due the discrepancy between caclulated and actual concentrations explained in Section 3.3. This effect had a particularly large impact between these test cells since the initial water content was twice as high for Calcigel bentonite with bacterial addition (+) than the bentonite fraction without any addition (−).

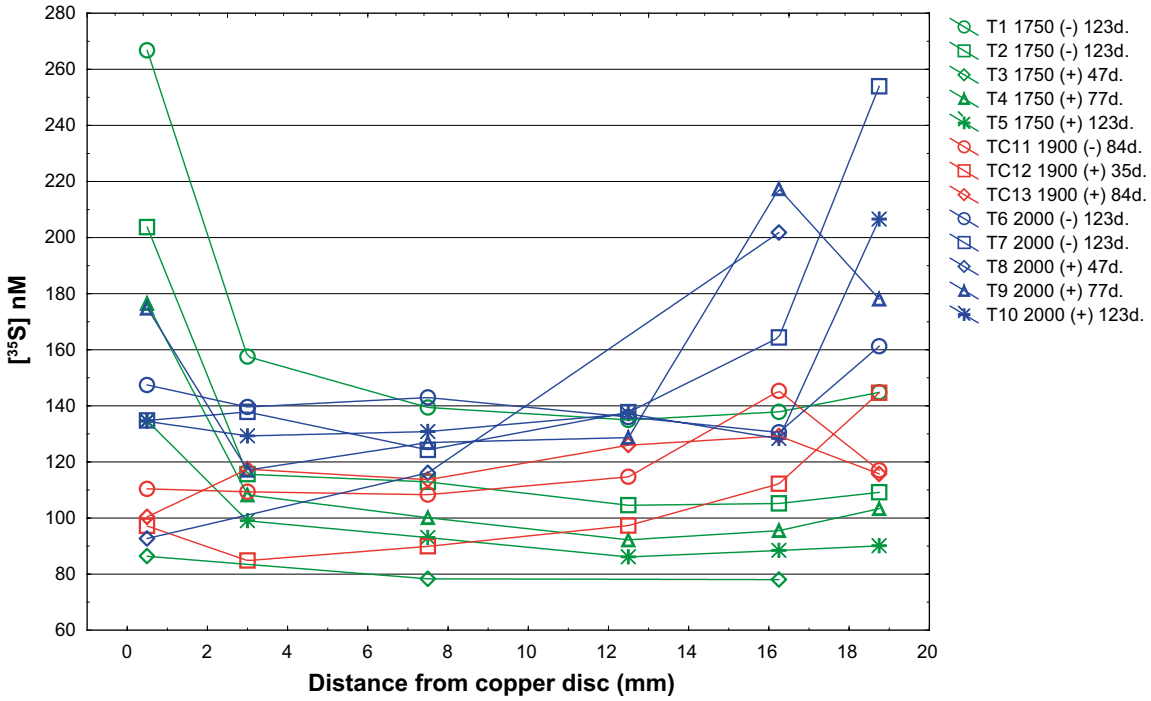

Figure 3-2. *Concentrations of ^{35}S in profiles in MX-80 bentonite cores for each test cell. Test cell number, bentonite density, addition of microbes (+/−) and incubation time according to symbol description.*

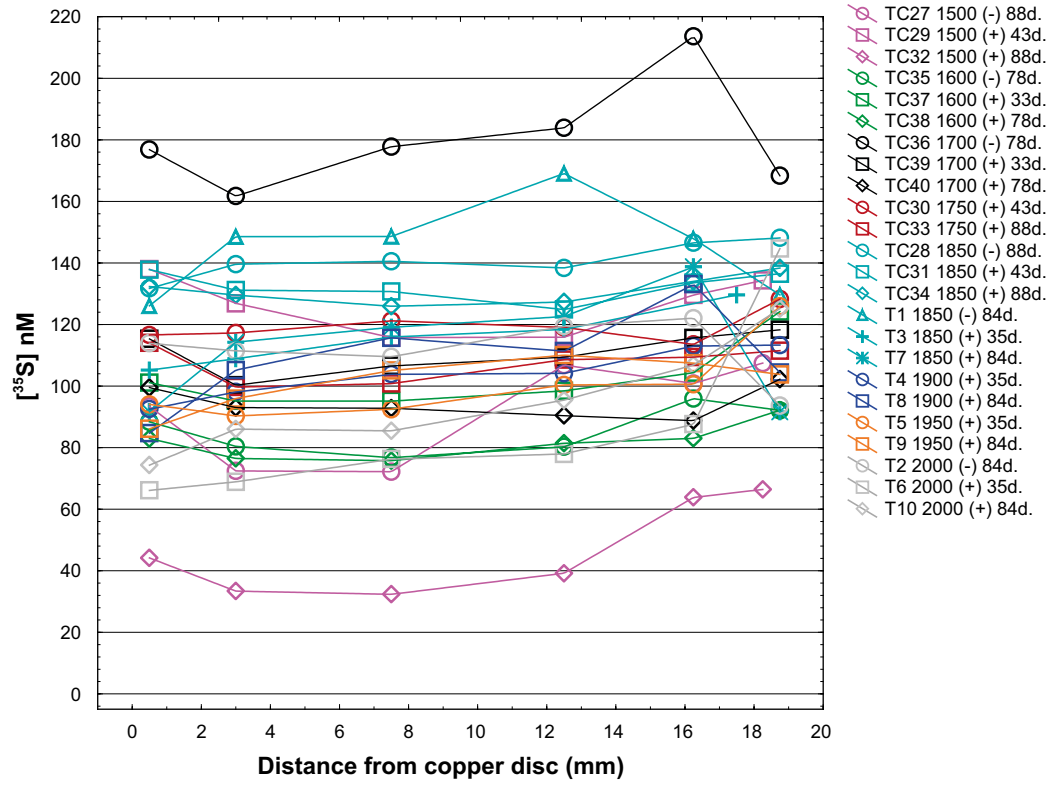

Figure 3-3. *Concentrations of ^{35}S in profiles in Asha bentonite cores for each test cell. Test cell number, bentonite density, addition of microbes (+/−) and incubation time according to symbol description.*

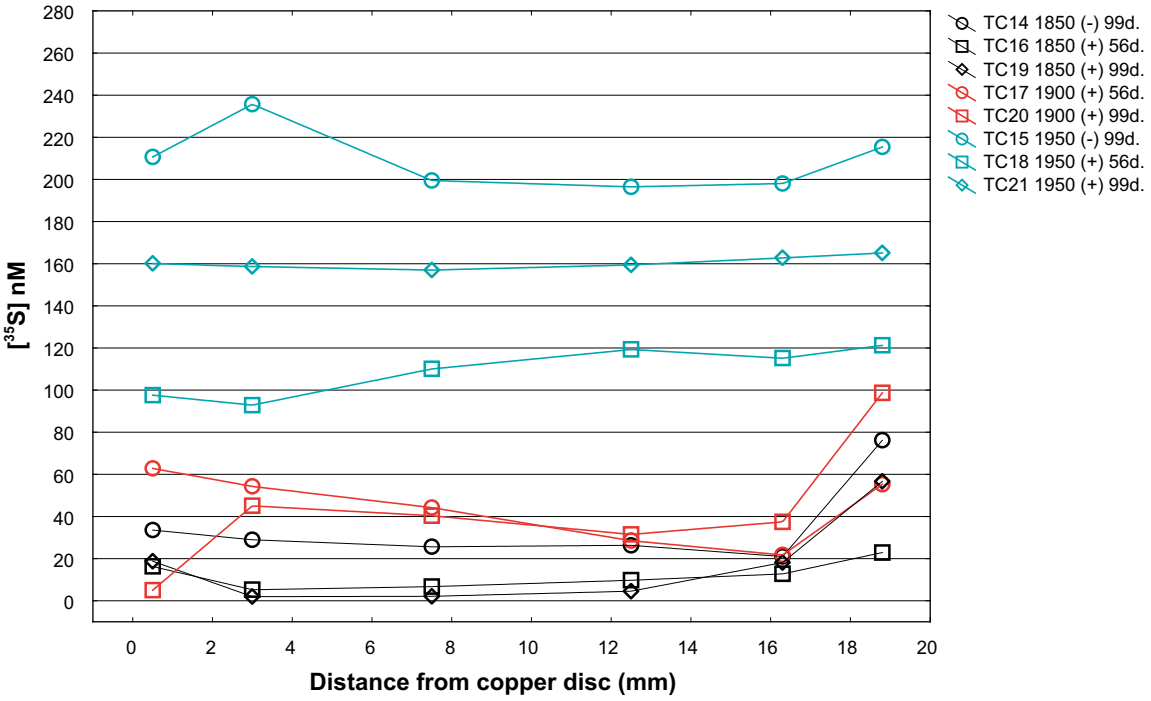

Figure 3-4. *Concentrations of ^{35}S in profiles in Calcigel bentonite cores for each test cell. Test cell number, bentonite density, addition of microbes (+/−) and incubation time according to symbol description.*

3.4 Distribution of SO_4^{2-} in the bentonite core

The average leachable amount of sulphate in raw, dry bentonite was determined for the three types of bentonites. MX-80 had 22 µmoles sulphate g^{-1} (SD ± 0.89, n=10), Asha had 38 µmoles sulphate g^{-1} (SD ± 4, n=3) (Table 3-7). Leachable sulphate was not detected in Calcigel samples. The amounts of sulphate in MX-80 and Asha were obtained for five different leaching volumes 10 to 50 mL, i.e. the amount of leachable sulphate was independent of the volume used to disperse the bentonite. A second batch of water did not result in more sulphate; all sulphate was leached in the first leaching cycle. This leaching experiment consequently demonstrated that there was an easily leachable fraction of sulphate in the MX-80 and Asha bentonites. Re-calculating these amounts of sulphate per g clay to pore water concentrations in the test cells returns 40–100 mM sulphate for Asha and 40–60 mM for MX-80; the concentration increases with increasing density. These amounts correspond reasonably well with literature values reported for MX-80 that were approximately up to 100 mM (Bradbury and Baeyens 2003, Muurinen and Lehikoinen 1999).

The distribution of leachable sulphate was non-uniform in many of the cores with low concentrations close to one or both ends of the clay cores except for test cells with a large $Cu_x{}^{35}S$ production (Figure 3-5 and Figure 3-6). The sulphate profiles were low at the inlet side in experiment 1 and low at both inlet sides in the remaining experiments that were water saturated from both sides. The medium used for water saturation contained 7 mM Ca^{2+}. During saturation, leachable sulphate may have been transported inwards in the clay cores and partly precipitated as gypsum as observed by Muurinen and Lehikoinen (1999). The solubility of gypsum is approximately 0.2 mM which suggests that most of the re-located sulphate might have been immobilised and not able to diffuse back to where it was transported from during the time course of the experiments.

Table 3-7. Leachable amount of sulphate in raw, dry bentonite.

Bentonite	Leachable amount of sulphate (µmoles gdw^{-1})
MX-80	22 (SD ± 0.89)
Asha	38 (SD ± 4)
Calcigel	< 2

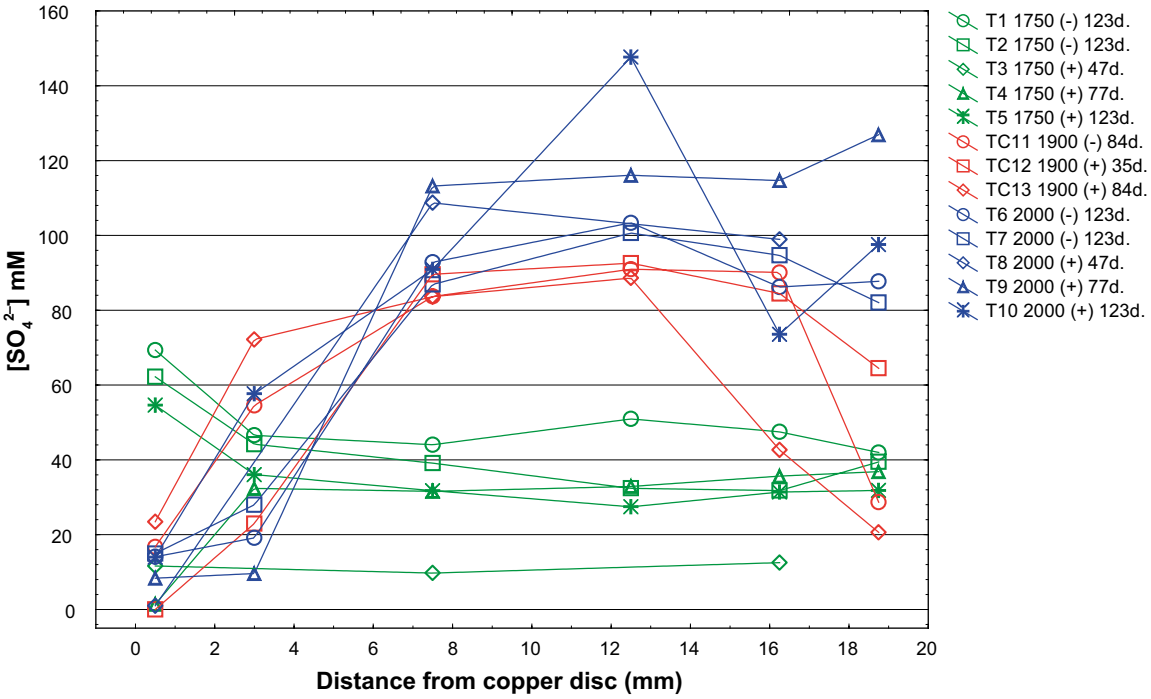

Figure 3-5. *Concentrations of sulphate in profiles of MX-80 bentonite cores for each test cell. Test cell number, bentonite density, addition of microbes (+/−) and incubation time according to symbol description.*

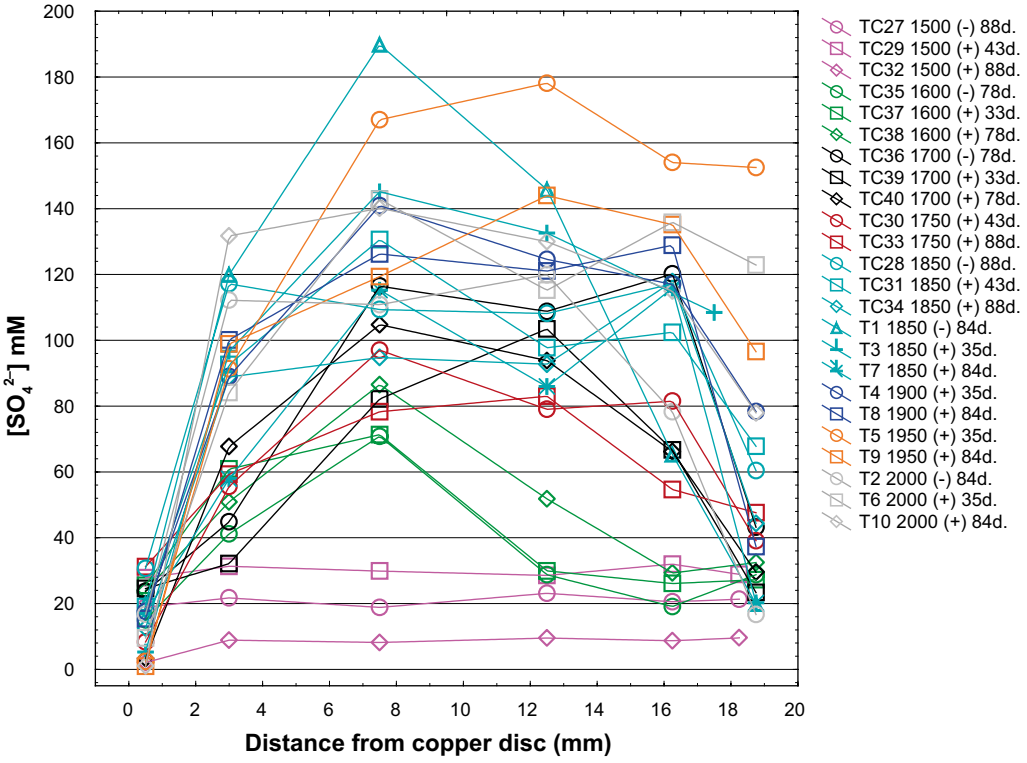

Figure 3-6. *Concentrations of sulphate in profiles of Asha bentonite cores for each test cell. Test cell number, bentonite density, addition of microbes (+/−) and incubation time according to symbol description.*

3.4.1 Average amounts of remaining sulphate in test cell pore water

The average concentrations of leachable sulphate for all test cells at the end of the experiments are shown over the total amounts of S on the copper discs in Figure 3-7. The average concentrations in test cells with no or small production of Cu_xS were not significantly different from the respective values of leachable sulphate from Asha and MX-80. For test cells with the largest amount of S on the copper discs, the average concentrations of sulphate were generally lower, or much lower than what was originally leachable. The decrease in concentrations of sulphate in these cells correlates positively with sulphide-production in the clay analysed as radioactivity on the copper discs, re-calculated to total amount of sulphur.

3.5 Rate of sulphate to sulphide reduction

Previously, we calculated diffusion coefficients for sulphide in compacted Wyoming MX-80 bentonite based on the transport of sulphide from sulphide-production activity to known S^{2-}concentrations in water outside the bentonite (Pedersen 2010). A relation between the wet density and the rate of diffusion was determined to be linear at 0.4×10^{-11} units per 100 kg m^{-3} wet density (approximately 75 kg m^{-3} dry density). This relation between density and diffusivity was used for both the sulphate and the sulphide diffusion coefficients starting with a coefficient of 2×10^{-12} m^2 s^{-1} for sulphate at a wet density of 2 000 kg m^{-3} and a dry density of 1 600 kg m^{-3}. The corresponding starting coefficient for sulphide was set to 4.0×10^{-12} m^2 s^{-1}.

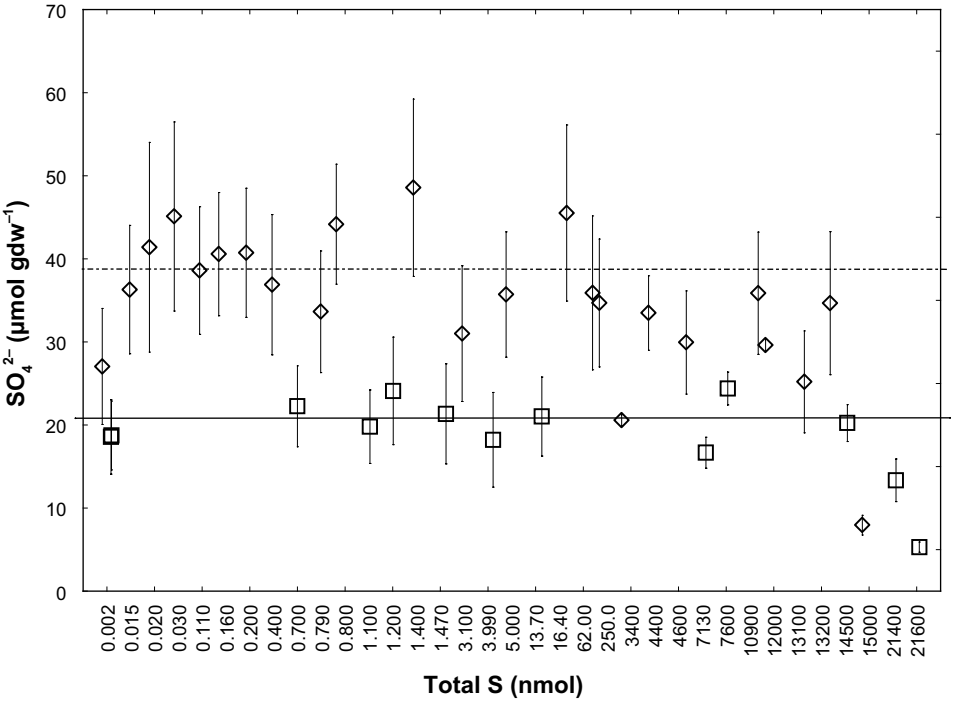

Figure 3-7. *The average amounts of sulphate in test cells for three different ranges of S on the copper discs. The broken line shows the leachable amount of sulphate in Asha bentonite and the solid line shows the leachable amount of sulphate in MX-80. Diamonds show average amount of leachable sulphate from Asha and squares shows amount of leachable sulphate from MX-80. Bars denote standard error. Total amounts of S were obtained from Table 3-1 and Table 3-2.*

3.5.1 MX-80

The choices of dT and the numbers of cells used to compute the results in Table 3-8 have been made so that the numerical accuracy of the calculations are at least an order of magnitude better than the uncertainty of the input data into the program. This is obvious when comparing the results for the same input data run with dT= 900 instead of 600 and $31 \times 31 \times 31$ cells instead of $51 \times 51 \times 51$. This was done as part of the sensitivity analysis for test cell 8 and the difference in result was minor, i.e. 6.2×10^{-9} and 6.3×10^{-9}, respectively. The sensitivity analysis (Table 3-9) demonstrated that increasing the diffusion coefficient for sulphide 3 orders of magnitude resulted in a 20 times decrease in the calculated reduction rate while a 3 orders of magnitude increase of the diffusion coefficient for sulphate returned a 7 times decrease in the reduction rate. The calculated rates were consequently 3 times more sensitive to the choice of diffusion coefficient for sulphide than for sulphate.

The rate of sulphate reduction for the MX-80 test cells from experiment 2 where no, or very small amounts of accumulated ^{35}S could be found on the copper discs, were not determined since the calculated reduction rate would be extremely slow or outside all reasonable detection limits as for test cell 6 and 7 in experiment 1. The implications of the calculated reduction rates are further treated in the discussion.

Table 3-8. Sulphate and sulphide diffusion coefficients and sulphate to sulphide reduction rates for all MX-80 test cells in experiment 1. For test cell 6 and 7 where no activity could be detected on the copper discs the detection limit for reduction rates are based on an imaginary value of 1 gross count (1 Bq). The theoretical amounts of reduced sulphate, were calculated based on the reduction rates.

Test cell code	Diffusion coefficient sulphate ($m^2\ s^{-1}$)	Diffusion coefficient sulphide ($m^2\ s^{-1}$)	Sulphate to sulphide reduction rate ($mol\ s^{-1}\ m^{-3}$)	Reduced sulphate (mM)
MX-80				
T3 1750 (+) 47d.	1.2×10^{-11}	2.4×10^{-11}	8.2×10^{-7}	11.2
T4 1750 (+) 77d.	1.2×10^{-11}	2.4×10^{-11}	3.2×10^{-7}	4.39
T5 1750 (+) 123d.	1.2×10^{-11}	2.4×10^{-11}	5.0×10^{-8}	1.01
T1 1750 (−) 123d.	1.2×10^{-11}	2.4×10^{-11}	5.5×10^{-8}	1.11
T2 1750 (−) 123d.	1.2×10^{-11}	2.4×10^{-11}	1.0×10^{-7}	2.10
T8 2000 (+) 47d.	2.0×10^{-12}	4.0×10^{-12}	6.1×10^{-9}	0.11
T9 2000 (+) 77d.	2.0×10^{-12}	4.0×10^{-12}	9.2×10^{-11}	0.002
T10 2000 (+) 123d.	2.0×10^{-12}	4.0×10^{-12}	3.2×10^{-10}	0.01
T6 2000 (−) 123d.	2.0×10^{-12}	4.0×10^{-12}	$< 3.7 \times 10^{-14}$	< 0.000001
T7 2000 (−) 123d.	2.0×10^{-12}	4.0×10^{-12}	$< 3.7 \times 10^{-14}$	< 0.000001

Table 3-9. Sensitivity analysis for variation of diffusion coefficients for sulphate and sulphide on the calculated sulphate to sulphide reduction rate ($mole\ s^{-1}\ m^{-3}$) applied on test cell 8. The used values and the resulting rate for the used coefficients are marked as bold.

Diffusion coefficient sulphate ($m^2\ s^{-1}$)	Diffusion coefficient sulphide ($m^2\ s^{-1}$)					
	1×10^{-10}	2×10^{-11}	1×10^{-11}	**4×10^{-12}**	2×10^{-12}	4×10^{-13}
1×10^{-10}	9.6×10^{-11}		2.9×10^{-10}		6.8×10^{-10}	1.6×10^{-7}
2×10^{-11}			3.0×10^{-10}		7.4×10^{-10}	2.1×10^{-9}
1×10^{-11}	9.9×10^{-11}	2.2×10^{-10}		5.6×10^{-10}		
4×10^{-12}			4.3×10^{-10}		1.4×10^{-9}	5.6×10^{-9}
2×10^{-12}	1.5×10^{-10}	5.0×10^{-10}		**6.1×10^{-9}**		
4×10^{-13}	6.8×10^{-10}	7.1×10^{-9}		2.1×10^{-5}		

3.5.2 Asha

The diffusion coefficients set for sulphate and sulphide as well as the sulphate to sulphide reduction rate for the three Asha test cells that had accumulated $Cu_x{}^{35}S$ on their copper discs is shown in Table 3-10. The reduction rates are comparable to the ones found for MX-80 except for test cell 29 that had approximately a hundred times faster reduction rate. Even though the diffusion coefficients for both sulphate and sulphide was set to the same values for test cell TC29 as for the other two calculated Asha cases the incubation time was half for this test cell compared to the other two test cells. Consequently, as the autoradiograph measurements resulted in comparable amounts of accumulated $Cu_x{}^{35}S$, even higher in test cell 29, the reduction rate becomes faster in that case. However, it seems unlikely that the reduction rate should differ between test cells with the same bentonite density and test cell 27 probably had the same amount of $Cu_x{}^{35}S$ accumulation also after 43 days as test cell 29 but since no sampling was performed at that time this assumption cannot be confirmed. Reduction rates and diffusion coefficient for the remaining Asha test cells that did not show any measurable microbial sulphate-reducing activity were not calculated due to the same issue as for MX-80 where the reduction rate would be very low and uncertain. The reduction rates and diffusion coefficients are further treated in the discussion.

Table 3-10. Sulphate and sulphide diffusion coefficients and sulphate to sulphide reduction rates for Asha test cells with activity above detection limit. The theoretical amounts of reduced sulphate, were calculated based on the reduction rates.

Test cell code	Diffusion coefficient sulphate ($m^2\ s^{-1}$)	Diffusion coefficient sulphide ($m^2\ s^{-1}$)	Sulphate to sulphide reduction rate ($mol\ s^{-1}\ m^{-3}$)	Reduced sulphate (mM)
Asha				
TC29 1500 (+) 43d.	2.2×10^{-11}	4.4×10^{-11}	6.3×10^{-6}	30.8
TC32 1500 (+) 88d.	2.2×10^{-11}	4.4×10^{-11}	1.3×10^{-7}	1.36
TC27 1500 (−) 88d.	2.2×10^{-11}	4.4×10^{-11}	3.0×10^{-8}	0.31

3.5.3 Calcigel

The diffusion coefficients set for sulphate and sulphide as well as the sulphate to sulphide reduction rate for the three Calcigel test cells that had accumulated $Cu_x{}^{35}S$ on their copper discs is shown in Table 3-11. The choice of diffusion coefficients is treated further in the discussion. The reduction rates for Calcigel were similar to those found for the other two bentonite types except for test cell 14 which had a very low accumulation of $Cu_x{}^{35}S$, however still above the detection limit, which then resulted in a slower reduction rate, as expected.

Table 3-11. Sulphate and sulphide diffusion coefficients and sulphate to sulphide reduction rates for Calcigel test cells with activity above detection limit. The theoretical amounts of reduced sulphate, were calculated based on the reduction rates.

Test cell code	Diffusion coefficient sulphate ($m^2\ s^{-1}$)	Diffusion coefficient sulphide ($m^2\ s^{-1}$)	Sulphate to sulphide reduction rate ($mol\ s^{-1}\ m^{-3}$)	Reduced sulphate (mM)
Calcigel				
TC16 1850 (+) 56d.	8.0×10^{-12}	1.6×10^{-11}	1.3×10^{-8}	0.117
TC19 1850 (+) 99d.	8.0×10^{-12}	1.6×10^{-11}	6.1×10^{-9}	0.093
TC14 1850 (−) 99d.	8.0×10^{-12}	1.6×10^{-11}	3.8×10^{-10}	0.006

4 Discussion

4.1 Experimental set-up

The experimental set-up was developed based on experiences from previous experiments using test cells made of stainless steel (Masurat et al. 2010, Pedersen 2010, Pedersen et al. 2000b). The test cells used in these experiments were made of titanium because this metal does not easily react with sulphide (Persson et al. 2011), which may be the case with stainless steel. Further, in earlier experiments, it was found that microbial sulphide-producing activity in free water adjacent to the bentonite cores became very intensive and the produced sulphide interfered with the analysis of the sulphide production rates inside the bentonite cores (Pedersen 2010). Therefore, the present experimental equipment was constructed to exclude any free water in contact with the bentonite cores after the addition of carbon sources and $^{35}SO_4^{2-}$. Any production of $Cu_x{}^{35}S$ in the present experiments must have originated from bacterial sulphate-reducing activity inside the bentonite cores.

The present set-up employed copper discs installed at one end of the bentonite core which differs from the preceding experiment where 1.6 cm^2 copper test plates (1 × 5 × 13 mm) were positioned in depth profiles of the bentonite core (Masurat et al. 2010, Pedersen 2010). The present configuration was a return to an older configuration where silver foils were installed at the end of the core (Pedersen et al. 2000b). The use of one large metal surface of 9.6 cm^2 compared to 4 smaller surfaces ($4 \times 1.6 = 6.4$ cm^2) was reasonably comparable with respect to the surface area. Both configurations will report similar total amounts of $Cu_x{}^{35}S$. However, the configuration with a bottom metal plate can be argued to more appropriately simulate a bentonite-copper-canister interface.

The knowledge of a strong relation between the density of the bentonite and survival and activity of microorganisms in compacted MX-80 bentonite was established a long time ago (Motamedi et al. 1996). It is likely that the density generated swelling pressure has an important role in the control of microbial activity in compacted bentonite. The wet density and the corresponding swelling pressure of a compacted bentonite core is determined by an invariable confined compaction space, amount and type of bentonite and water saturation. Previously, swelling pressure was set by water saturation of bentonites at different densities in test cells and the actual pressure could not be registered. In the present experiment, the test cells were installed with force transducers that precisely reported pressures throughout the experiments.

The radioactive isotope ^{35}S was used as a tracer for microbial sulphide-producing activity in these experiments. Because this isotope has a short half-life of only 87.4 days it constitutes a very sensitive tracer for microbial sulphide production. This isotope has, therefore, been successfully used for studies of microbial sulphide production in marine sediments for several decades (Jørgensen 1978). From stable isotope studies, in pure cultures and in the field, it has been found that the light isotope, $^{32}SO_4^{2-}$ is metabolized faster than $^{35}SO_4^{2-}$. The relative discrimination against $^{35}SO_4^{2-}$ will depend on the species of SRB present, growth conditions and available substrates (Brüchert et al. 2001). Typically, the fractionation factor, α, can be 1.05–1.06 (Rudnicki et al. 2001). The enrichment factor, ε, vary similarly depending on the concentrations of $^{32}SO_4^{2-}$ and $^{35}SO_4^{2-}$ at start and end of a growth period if the system is closed without an external supply of SO_4^{2-} (Detmers et al. 2001). The fractionation factor was not known for the SRB populations under the conditions they encountered in the studied bentonite cores. Therefore, the data were not compensated for a possible fractionation of $^{32}SO_4^{2-}/^{35}SO_4^{2-}$ which means that the modelled rates may have been underestimated by a couple of percent. However, this work was designed to compare microbial sulphide-producing activity under varying wet densities was the only independent variable applied. All other conditions, concentrations of electron donors, acceptors, temperatures and carbon sources were kept constant. A similar α factor can, therefore, be anticipated for all test cells where the added SRB dominated the sulphide production and comparisons of microbial activity over density and pressure will be valid.

During the progression of the 5 experimental series (Table 2-1) some improvements of the methodologies were introduced. The number of subsampled layers per bentonite core was doubled from 3 to 6 after sampling and analysis of the two first test cells (Figure 2-8). This change increased the spatial resolution of the distribution of sulphur species significantly (Figure 3-2). The evaluation of experiment 1 with MX-80 suggested that there was a narrow slit between the titanium cylinder and

the copper discs which resulted in a higher sulphide-producing activity than expected for the highest densities (Bengtsson et al. 2015). The way around this problem was to exclude the radioactivity data generated by this edge effect in the analysis of data. The titanium and copper discs were modified with a bevelled edge that enabled the bentonites to swell uniformly around the edges. The edge effect did not appear during experiments 2–5.

The water saturation of the bentonites was performed from one side of the core during experiment 1. It was found that sulphate was redistributed by the water flow into the bentonite (Figure 3-5). The following experimental configurations were changed to a set-up with water saturation from both sides of the bentonite core which reduced the redistribution effect significantly. The process of water saturation and build-up of planned swelling-pressures was modified as well during the course of the experiments. In experiment 1, the Allen screws of the test cell were continuously adjusted until the planned swelling pressures were obtained. These adjustments were performed with free transport of water in and out of the bentonite in test cells for a period of approximately 20 days until addition of isotopes and copper discs (Figure 6-1 and Figure 6-2). Consequently, the registered pressures in experiment 1 were generated by the swelling capacity of the bentonite. Still, this procedure was not regarded optimal and experiments 2–5 were modified. Fixed distance spacers were installed and adjustments were not done. The resulting swelling pressures did drop off somewhat during the course of the experiments with Asha and MX-80 but were stable with Calcigel (see Appendix 6.1).

In summary, the present experimental set-up has passed through a large number of development steps, starting two decades ago with blunt steel test cells and silver foils. A series of different technical approaches have been tested since then using both addition of pure cultures of SRB in the laboratory (Motamedi et al. 1996, Pedersen et al. 2000a, b), in situ addition of SRB present in groundwater at Äspö hard rock laboratory (Masurat et al. 2010, Pedersen 2010) and control experiments without additions of SRB. The control experiments without added SRB have repeatedly demonstrated the presence of inherent SRB in the bentonites. There were advantages and disadvantages with the previous set-ups but the equipment and experimental procedures presented in this report enable detailed and controlled experiments on the activity of sulphide-producing bacteria in compacted bentonite as a function of a large array of independent variables such as electron donor and acceptor, temperature, carbon source, species of microorganisms, type of bentonite, groundwater composition and density.

4.2 Survival and cultivability of sulphate-reducing bacteria

The experiments relied on two different sources of SRB. Selected test cells were loaded with bentonites doped with three different species of SRB. Test cells without doped bentonites had inherent populations of SRB. Heat sterilisation of control bentonites was unsuccessful in several cases and resulted in significant sulphide production from heat-resistant SRB. The three added SRB were selected to cover representative SRB with different capabilities to survive extreme conditions and grow in deep groundwater and bentonite.

Desulfovibrio aespoeensis was isolated from deep groundwater (Motamedi and Pedersen 1998) This species is typical for deep groundwater and consequently represent SRB that may enter the bentonite buffer from groundwater during the saturation phase. DNA evidence for the presence of this SRB was found on the copper canisters in the prototype experiment (Arlinger et al. 2013). The full genome is sequenced which can be helpful when knowledge about metabolic traits and pathways is required (Pedersen et al. 2014b). *Desulfotomaculum nigrificans* is a Gram-positive, thermophilic, spore-forming sulphide-producing bacterium. Gram-positive spore-forming sulphate reducers and particularly members of the genus *Desulfotomaculum* are commonly found in the subsurface biosphere by culture based and molecular approaches (Aüllo et al. 2013). Due to their metabolic versatility and their ability to persist as endospores *Desulfotomaculum* spp. are well-adapted for colonizing SNF repository environments from groundwater and they have been found in the buffer-rock interface in full scale experiments at Äspö HRL (Arlinger et al. 2013) and in MX-80, Friedland, FEBEX, Ikosorb and Ibeco Seal bentonites (Svensson et al. 2011). *Desulfosporosinus orientis* is spore-forming, mesophilic sulphide-producing bacterium with the ability to grow with H_2 as source of energy; full

genome is sequenced (Stackebrandt 2014, Stackebrandt et al. 2003). This bacterium is related to *Desulfotomaculum* but is not thermophilic. All three added SRB species are so called incomplete oxidizers of lactate. They all oxidize lactate to acetate that is not further metabolized.

The diversity and metabolic capabilities of the inherent SRB that follow the bentonites from their producers are not possible to describe in detail. Little is known at present because it is difficult to separate microorganisms from sediments and clays, in particular bentonites (Kallmeyer and Smith 2009, Kallmeyer et al. 2008). Recently bentonite samples were collected from clay formations from three different sites in Almeria bentonite (source for FEBEX), in the south-east of Spain and sequenced (Lopez-Fernandez et al. 2015). The results indicated a large diversity of microorganisms. *Desulfosporosinus,* a sulphate-reducing Gram positive bacterium, was found in bentonite from the long term tests (LOT) of bentonite and from the canister retrieval tests in the Äspö HRL tunnel (Chi Fru and Athar 2008).

In the currently planned SNF repository concept, the maximum surface temperature of the copper canisters may not exceed 90 °C. In an earlier experiment, heat treatment at 120 °C for 15 h failed to kill inherent bacteria in the bentonite (Masurat et al. 2010). There was a heat treatment of the bentonite at 110 °C for 170 h in experiment 1 intended to sterilize the bentonite from bacteria; prolonged exposure to heat was expected to be efficient. Obviously this was still not enough to kill off SRB in the bentonite because intensive sulphide-producing activity and large numbers of cultivable SRB were observed in the MX-80 1 750 kg m^{-3} control test cells with heat treated bentonite but not in the MX-80 control test cells at densities 1 900 kg m^{-3} or higher (Table 3-4). It should be noted that the heat treated bentonites were not added with SRB; all sulphide was produced by SRB that survived the heat treatment. One explanation to the heat-survival could be the presence of spores from spore-forming SRB. Heat-tolerant bacterial spores can survive heat treatment and later be activated by exposure to the groundwater used. The presence of spores would also explain viable SRB originating from dry bentonites with only 10% water content and two of the added SRB may have developed spores in the cultures. Alternatively, bentonite or rather montmorillonite, has a verified high affinity for water and the cell membrane of bacterial cells is water permeable. If a bacterial cell is surrounded by bentonite, it is possible that the water affinity of montmorillonite will extract water from the cell, leaving it in a desiccated state. The phenomenon of drying cells for prolonged disposal is well known and commonly used in microbiology (Gherna 1994). Slow desiccation can yield higher viability, after prolonged disposal, than can fast desiccation (Laroche and Gervais 2003, Potts 1994) and also increased heat resistance and viability for both spores and vegetative cells (Fine and Gervais 2005). The heat treatment was abandoned in experiment 2–5 and intensive sulphide-producing activity and large numbers of cultivable SRB were observed in the Asha 1 500 and 1 600 kg m^{-3} test cells without added SRB (Table 3-5) but not in the Asha bentonite at densities at 1 700 kg m^{-3} or higher without added SRB. The Calcigel 1 850 kg m^{-3} negative control without added SRB showed increased sulphide-producing activity as well. Consequently, it is obvious that the commercial bentonites all were infested with inherent, viable and cultivable SRB that were activated in the experiments. At present, it is not possible to conclude which SRB produced the sulphide in the experiments; it might have been the added SRB, the inherent SRB or a mixture of added and inherent species, except for the non-added controls with only inherent SRB.

Previously, it has repeatedly been shown that cultivability of bacteria in compacted bentonite was negatively correlated with increasing density (Masurat et al. 2010, Pedersen 2010). The present results corroborate this correlation for MX-80 and Calcigel but not for Asha where the numbers of cultivable SRB were constant at densities above 1 700 kg m^{-3} (Figure 3-1). Based on previous and present results, it appears safe to conclude that microbial cultivability was strongly reduced when the wet density approaches 1 900 kg m^{-3} in MX-80 and Calcigel. However, it must be taken into account that the data is based on cultivation. It is generally accepted that far from all microbial diversity can be cultivated. Consequently, there seems not to exist a precise cut-off density for when microorganisms in highly compacted bentonite is completely eradicated. The relation between density and microbial cultivability varied with the type of bentonite at similar densities and swelling pressures for unknown reasons that need to be further investigated for a full understanding of factors that control survival of SRB in compacted bentonite clays.

4.3 Accumulation of $Cu_x^{35}S$ on copper discs

The accumulations of $Cu_x^{35}S$ over wet density of the bentonite for copper discs fitted in test cells with bacterial additions from experiment 1 to 5 are displayed in Figure 4-1. For each bentonite type there was a relatively small interval in wet density in which sulphide-producing activity registered as $Cu_x^{35}S$ dropped from high to very low or to absence of $Cu_x^{35}S$. The present range of each interval may just be a matter of the number of sampling points and the selected densities; analysis of more densities may possibly narrow the range. The analysed wet density where the formation of $Cu_x^{35}S$ had dropped to a very low value were similar for Calcigel and MX-80 at 1 870 kg m^{-3} wet density (Figure 4-1). The corresponding value for Asha was lower, at 1 830 kg m^{-3}. Consequently, there may be at least one more additional factor to wet density that influence microbial activity in compacted bentonites to fully explain the difference in these values between Asha compared to MX-80 and Calcigel. This factor, or factors, are probably nested within the different bentonites types.

The swelling pressure in the bentonite originates from separating flocs in the bentonite. This means that a mechanical pressure arises between the separating flocs, approximately equal to the swelling pressure. Even in low-density bentonites (1 500 kg m^{-3}), a pore size in the nm range would theoretically not allow for bacterial existence unless the bacteria could withstand the mechanical pressure from the separating flocs (0.09 MPa at 1 500 kg m^{-3}). Prokaryotic cells can compensate for the mechanical pressure in compacted bentonite by turgor pressure. Published data on turgor pressure in prokaryotic cells mention pressures between 0.08 MPa and 2 MPa (Potts 1994). An upper limit of 2 MPa turgor pressure would mean that cell integrity is possible, though limited, at bentonite swelling pressures below 2 MPa. The range of the observed RSPs intervals where sulphide-producing activity dropped close to the detection limits were 0.5–0.8 MPa, which is lower than the theoretical threshold of 2 MPa discussed above. Far from all prokaryotic cells can produce a turgor pressure of 2 MPa. Note that endospores can survive a much higher pressure but spores are inactive and do not produce sulphide. An investigation similar to the work presented here investigated Boom Clay where a mechanical load replaced the pressure generated by the montmorillonites (Bengtsson and Pedersen 2016). There was a low but significant sulphide-producing activity in the Boom Clay up to the highest load tested, i.e. 2.5 MPa.

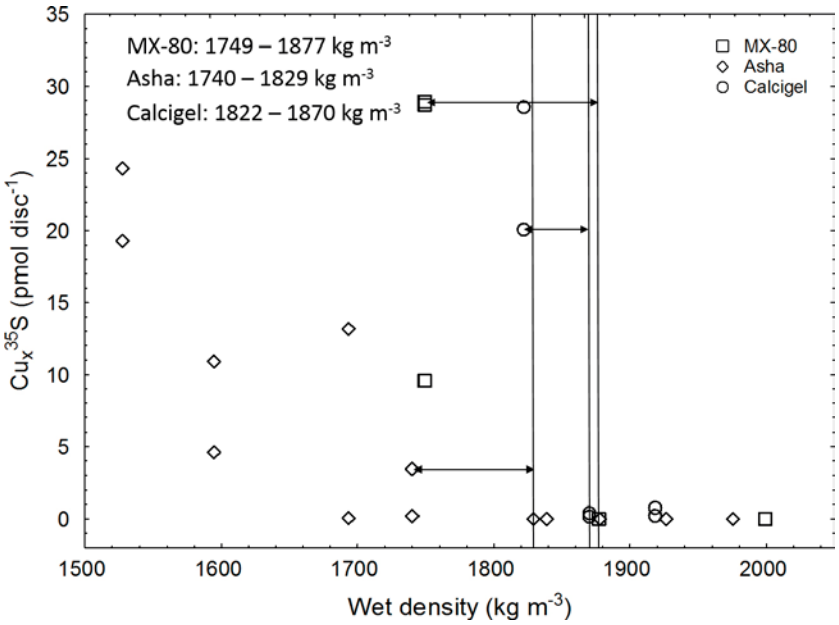

Figure 4-1. *Accumulated $Cu_x^{35}S$ on copper discs (pmol) over wet density. The respective intervals where sulphide-production shifts from high to low are indicated with arrows. The corresponding analysed wet densitiy intervals are inserted.*

4.4 Transport of sulphate, sulphide and lactate in bentonites

The interpretation of the results and the modelling of sulphide production rates rely profoundly on our understanding of transport rates of sulphate, sulphide and lactate in compacted bentonites. The output from modelling of bacterial sulphide-production rates in the bentonite cores (Table 3-8, Table 3-10 and Table 3-11) depends on the choice of diffusion coefficients. There was some uncertainty about the values for sulphate and sulphide because the literature is fairly short on such values, particularly for sulphide ions and hydrogen sulphide while some values can be found for sulphate. In a work investigating gypsum dissolution, the actual/apparent diffusion coefficient for sulphate in a sodium Wyoming bentonite (dry density 1 460 kg m^{-3}) was determined to 4.2×10^{-12} m^2 s^{-1} (Birgersson et al. 2009). The calculated value for diffusion coefficient for sulphate in FEBEX bentonite (dry density 1 650 kg m^{-3}) was also 4.2×10^{-12} m^2 s^{-1} (García-Gutiérrez et al. 2006). In a work using radioactive $^{35}S^{2-}$, the diffusivity of HS^- was found to be to 9×10^{-12} m^2 s^{-1} and to 4×10^{-12} m^2 s^{-1} in MX-80 and Bavarian Erbslöh calcium bentonites, respectively, at 2 100 kg m^{-3} wet density (Eriksen and Jacobsson 1982). Previously, we calculated diffusion coefficients for sulphide in compacted Wyoming MX-80 bentonite based on the transport of sulphide from sulphide-production activity to known sulphide concentrations in water outside the bentonite (Pedersen 2010). The coefficient for sulphide in Wyoming MX-80 at a wet density of 2 000 kg m^{-3} became 2×10^{-12} m^2 s^{-1} which is approximately 50 % slower than the rate used in this work for bentonite cores at a wet density of 2 000 kg m^{-3}. A relation between the wet density and the rate of diffusion was determined to be linear at 0.4×10^{-11} units per 100 kg m^{-3} wet density (approximately 75 kg m^{-3} dry density). This relation between density and diffusivity was used for both the sulphate and the sulphide diffusion coefficients starting with a coefficient of 2×10^{-12} m^2 s^{-1} for sulphate at a wet density of 2 000 kg m^{-3} and a dry density of 1 600 kg m^{-3}. That number compare well with the number of 4.2×10^{-12} m^2 s^{-1} at a dry density of 1 460 kg m^{-3} taking the relation between density and rate into consideration, although an exact match may not apply due to different experimental configurations. It was assumed that sulphide diffused with a rate that was twice that of sulphate. The smaller diffusion coefficient, the faster sulphide-producing activity must be modelled in the bentonite to obtain the observed radioactivity on the copper surfaces as demonstrated by the sensitivity analysis results (Table 3-9).

The molar weight of the monovalent anion lactate is 90.1 g mol^{-1} which is somewhat lighter than the molar weight for the divalent anion sulphate (96.1 g mol^{-1}). The diffusivity for lactate is approximated to that of sulphate meaning that lactate will move through the bentonite with approximately the same rate as the added $^{35}SO_4^{2-}$. Heavier anions, 290–300 000 g mol^{-1}, were previously demonstrated to move slower, but they were all with ring structures (Eriksen and Jacobsson 1982). Lactate is a straight 3-carbon chain anion and consequently both lighter and less bulky than the tested heavier anions and should move faster.

4.5 Modelling of sulphide production rates

The amounts of Cu_xS on the copper discs over time were used to calculate sulphide production rates in the respective bentonite. The output from the model shows the sulphide production rates that must have taken place to explain the observed Cu_xS on the discs with the assumed diffusion rates. A second approach, albeit a bit coarse is to calculate the sulphide production rate from the consumed sulphate in the bentonite cores with significant sulphide production (≈ 14 mM) and model the corresponding amount of of Cu_xS that should be found on the copper discs.

The rate of sulphate to sulphide reduction calculated from Cu_xS on the copper discs decreased over incubation time for all tested densites. There can be several reasons for this result. Firstly, if the numbers of viable SRB decreased over time, the corresponding sulphide-producing activity would decrease. However, the cultivation results did not show any obvious decreasing trends in MPN of SRB over time in Asha but did so in the other two investigated bentonites. Secondly, the observed redistribution of sulphate may locally have decreased the isotope dilution factor somewhat. This could occur if the $^{35}SO_4^{2-}$ diffused faster towards the copper surface than the relocated sulphate did, something that is indicated by the analysis results of ^{35}S and sulphate distributions. Then more $H^{35}S^-$ would be produced close to the copper surface than what was calculated with the expected isotopic dilution. Over time, when redistributed sulphate has equalized again in the bentonite, this

effect will diminish. The distribution data of sulphate indicate that the equalization of sulphate concentrations in the bentonite occurred faster at low densities than at high densities. Thirdly, a more or less clear increase in ^{35}S close to the copper surfaces was observed for test cells with high sulphide production rates, most obvious for MX-80 and minor in the case of Calcigel. It may consequently be that some of the produced sulphide did not stay on, or reached, the copper discs but was located in the bentonite layer closest to the copper discs, which indeed had a black appearance nearby to the copper discs. That would have underestimated the sulphide production because it was only ^{35}S on the copper discs that was accounted for in the modelling. If this was the case, the modelling will predict a lower sulphide production rate in the bentonite than what was actually the case. Finally, if all sulphide production occurred rapidly in the test cells, before the first sampling occasion, the rates will decrease over time because the same amount of produced Cu_xS is divided by increasing values of time, as discussed next.

The amount of Cu_xS did not increase, or increased only to a limited extent, after the first sampling and analysis occasion at most tested densities where significant sulphide-production was observed, i.e. below the wet density interval where that activity diminished (Figure 4-1). This indicates that most, or all of the sulphide production in active sulphide producing test cells took place before the first sampling occasion. It seems possible to suggest that SRB rapidly produced approximately 14 mM sulphate within approximately 30 days in all test cells below the swelling pressure cut-off interval. Then, the modelled sulphide production rates will only be valid for the first analysed test cell in each time series. Modelling the following test cells in the time series will calculate rates based on the same total amount of produced sulphide, but for a longer period of time and, therefore, output smaller values than for the first sampling occasion. Copper discs in test cells with compaction to densities above the respective threshold wet density intervals had very low amount of Cu_xS, often unevenly distributed to small "hot spots". Because sulphate and lactate were present in excess in these test cells sulphide-producing activity would be theoretically possible throughout the experimental time. There were, however, no obvious increases in the observed Cu_xS values over time. Minor sulphide-production rates cannot be excluded, but if there were such microbial activity above the wet density threshold interval it was too small to validate within the time frame applied.

When the expected amounts of Cu_xS on the copper discs in test cells below the threshold values were modelled based on reduction of 14 mM sulphate to sulphide within 30 days there was too little Cu_xS accounted for on the copper discs. With the used diffusivities for sulphate to sulphide, there should have been more Cu_xS on the discs. At least two conceptual explanations to this discrepancy. The first explanation regards the assumed diffusion coefficients may be wrong. A manual fitting of a large combination of different coefficients for the Asha test cell 27 suggested 6.5×10^{-13} for sulphate and 3.7×10^{-12} for sulphide. With these diffusivities, the reduction rate in the bentonite did explain the observed amount of Cu_xS on the copper disc. These values are extreme compared to the used constants and the literature values and they stress the importance of having correct values for diffusivity. It is straight forward to experimentally determine these values as was demonstrated elsewhere for sulphate (Bengtsson and Pedersen 2016) and sulphide (Eriksen and Jacobsson 1982). The second explanation is on the interaction between sulphide and bentonites. If there is a sulphide retardation capacity in the bentonites that reduce transport rate and/or the amount of sulphide transported, less sulphide would reach the copper disc than modelled based on sulphate-reduction in the bentonites. That type of effect should be fairly straightforward to test experimentally as well by exposing bentonites to varying concentrations of sulphide and analyse distribution ratios for free and any immobilised sulphide in bentonite slurries and cores.

The sulphide producing activity must have been much larger in the bentonites than indicated by the copper discs, at least for MX-80 at 1 750 kg m^{-3} and Calcigel at 1 850 kg m^{-3} where modelling suggested 32 and 64 times larger rates in the bentonite based on disappearance of sulphate, respectively. For Asha at 1 500 kg m^{-3}, the difference was only 3 times after the first sampling occasion. The retarding effect appears to be density related, but the data set with one single observation for each clay is too small for significant conclusions and, therefore, only indicative.

Table 4-1. Sulphate to sulphide reduction rates for test cells with microbial sulphide-producing activity calculated from the amounts of accumulated $Cu_x{}^{35}S$ on copper discs and from the assumed reduction of 14 mM sulphate during the first 30 days.

Test cell code	Diffusion coefficient sulphate ($m^2\ s^{-1}$)	Diffusion coefficient sulphide ($m^2\ s^{-1}$)	Sulphate to sulphide reduction rate (mol $s^{-1}\ m^{-3}$)		Sulphate$^-$ to sulphide/Cu_xS
			Cu_xS	SO_4^{2-} to S^{2-}	
Asha					
TC29 1500 (+) 43d.	2.2×10^{-11}	4.4×10^{-11}	6.3×10^{-6}	1.4×10^{-5}	2.2
MX-80					
T3 1750 (+) 47d.	1.2×10^{-11}	2.4×10^{-11}	8.2×10^{-7}	3.1×10^{-5}	38
Calcigel					
TC16 1850 (+) 56d.	8.0×10^{-12}	1.6×10^{-11}	1.3×10^{-8}	8.7×10^{-7}	67

4.6 Conclusions

This work demonstrated that there are threshold bentonite wet densities for MX-80, Asha and Calcigel above which microbial sulphide-producing activity was practically inhibited with all others conditions being favourable for growth of SRB. The sulphide-production results for the three clays indicated intervals between 1 740–1 880 kg m^{-3} in wet densities within which sulphide-producing activity dropped from high to very low or below detection. The work also showed that cultivability of SRB from MX-80 and Calcigel decreased as a function of increasing densities. In opposite, the numbers did not decrease from Asha. Maintaining a high wet density of bentonite buffers in future SNF repositories may consequently significantly reduce the risk for sulphide corrosion of metal canisters.

References

SKB's (Svensk Kärnbränslehantering AB) publications can be found at www.skb.com/publications.

Arlinger J, Bengtsson A, Edlund J, Eriksson L, Johansson J, Lydmark S, Rabe L, Pedersen K, 2013. Prototype repository – Microbes in the retrieved outer section. SKB P-13-16, Svensk Kärnbränslehantering AB.

Aüllo T, Ranchou-Peyruse A, Ollivier B, Magot M, 2013. *Desulfotomaculum* spp. and related gram-positive sulfate-reducing bacteria in deep subsurface environments. Front Microbiol 4, 362.

Bengtsson A, Pedersen K, 2016. Microbial sulphate-reducing activity over load pressure and density in water saturated Boom Clay. Applied Clay Science 132–133, 542–551.

Bengtsson A, Edlund J, Hallbeck B, Heed C, Pedersen K, 2015. Microbial sulphide-producing activity in MX-80 bentonite at 1 750 and 2 000 kg m^{-3} wet density. SKB R-15-05, Svensk Kärnbränslehantering AB.

Birgersson M, Börgesson L, Hedström M, Karnland O, Nilsson U, 2009. Bentonite erosion. Final report. SKB TR-09-34, Svensk Kärnbränslehantering AB.

Bradbury M H, Baeyens B, 2003. Porewater chemistry in compacted re-saturated MX-80 bentonite. Journal of Contaminant Hydrology 61, 329–338.

Brüchert V, Knoblauch C, Jørgensen B B, 2001. Controls on stable sulfur isotope fractionation during bacterial sulfate reduction in Arctic sediments. Geochimica et Cosmochimica Acta 65, 763–776.

Chi Fru E, Athar R, 2008. In situ bacterial colonization of compacted bentonite under deep geological high-level radioactive waste repository conditions. Applied Microbiology and Biotechnology 79, 499–510.

Coulson J M, Richardson J F, 1990. Chemical engineering. 4th ed. Oxford: Pergamon.

Detmers J, Brüchert V, Habicht K S, Kuever J, 2001. Diversity of sulfur isotope fractionations by sulfate-reducing prokaryotes. Applied and Environmental Microbiology 67, 888–894.

Eriksen T, Jacobsson A, 1982. Diffusion of hydrogen, hydrogen sulfide and large molecular weight anions in bentonite. SKBF/KBS 82-17, Svensk Kärnbränsleförsörjning AB.

Fine F, Gervais P, 2005. Thermal destruction of dried vegetative yeast cells and dried bacterial spores in a convective hot air flow: strong influence of initial water activity. Environmental Microbiology 7, 40–46.

García-Gutiérrez M, Cormenzana J L, Missana T, Mingarro M, Molinero J, 2006. Overview of laboratory methods employed for obtaining diffusion coefficients in FEBEX compacted bentonite. Journal of Iberian Geology 32, 37–53.

Gherna R L, 1994. Culture preservation. In Gerhardt P, Murray R G E, Willis A W, Noel R K (eds). Methods for general and molecular bacteriology. Washington, DC: American Society for Microbiology, 278–292.

Greenberg A E, Clesceri L S, Eaton A D, 1992. Estimation of bacterial density. In Eaton A E, Clesceri L S, Rice E W, Greenberg A E (eds). Standard methods for the examination of water and wastewater 18. Washington: American Public Health Association, 9–49.

Hallbeck L, 2014. Determination of sulphide production rates in laboratory cultures of the sulphate reducing bacterium *Desulfovibrio aespoeensis* with lactate and H_2 as energy sources. SKB TR-14-14, Svensk Kärnbränslehantering AB.

Hallbeck L, Pedersen K, 2012. Culture-dependent comparison of microbial diversity in deep granitic groundwater from two sites considered for a Swedish final repository of spent nuclear fuel. FEMS Microbiology Ecology 81, 66–77.

Herbert H-J, Moog H C, 2002. Untersuchungen zur Quellung von Bentoniten in hochsalinaren Lösungen. Abschlussbericht GRS – 179. Gesellschaft für Anlagen und Reaktorsicherheit (GRS) mbH, Köln, Germany.

Hobbie J E, Daley R J, Jasper S, 1977. Use of nuclepore filters for counting bacteria by fluorescence microscopy. Applied and Environmental Microbiology 33, 1225–1228.

Jørgensen B B, 1978. A comparison of methods for the quantification of bacterial sulfate reduction in coastal marine sediments. I. Measurement with radiotracer techniques. Geomicrobiology Journal 1, 11–27.

Kallmeyer J, Smith D C, 2009. An improved electroelution method for separation of DNA from humic substances in marine sediment DNA extracts. FEMS Microbiology Ecology 69, 125–131.

Kallmeyer J, Smith D C, Spivack A J, D'Hondt S, 2008. New cell extraction procedure applied to deep subsurface sediments. Limnology and Oceanography: Methods 6, 236–245.

Karnland O, 2010. Chemical and mineralogical characterization of the bentonite buffer for the acceptance control procedure in a KBS-3 repository. SKB TR-10-60, Svensk Kärnbränslehantering AB.

Karnland O, Olsson S, Nilsson U, 2006. Mineralogy and sealing properties of various bentonites and smectite-rich clay materials. SKB TR-06-30, Svensk Kärnbränslehantering AB.

Karnland O, Olsson S, Dueck A, Birgersson M, Nilsson U, Hernan-Håkansson T, Pedersen K, Nilsson S, Eriksen T E, Rosborg B, 2009. Long term test of buffer material at the Äspö Hard Rock Laboratory, LOT project. Final report on the A2 test parcel. SKB TR-09-29, Svensk Kärnbränslehantering AB.

Laroche C, Gervais P, 2003. Unexpected thermal destruction of dried, glass bead-immobilized microorganisms as a function of water activity. Applied and Environmental Microbiology 69, 3015–3019.

Lopez-Fernandez M, Cherkouk A, Vilchez-Vargas R, Jauregui R, Pieper D, Boon N, Sanchez-Castro I, Merroun M L, 2015. Bacterial diversity in bentonites, engineered barrier for deep geological disposal of radioactive wastes. Microbial Ecology 70, 922–935.

Lydmark S, Pedersen K, 2011. Äspö Hard Rock Laboratory. Canister retrieval test. Microorganisms in buffer from the canister retrieval test – numbers and metabolic diversity. SKB P-11-06, Svensk Kärnbränslehantering AB.

Masurat P, Eriksson S, Pedersen K, 2010. Microbial sulphide production in compacted Wyoming bentonite MX-80 under *in situ* conditions relevant to a repository for high-level radioactive waste. Applied Clay Science 47, 58–64.

Morton K W, Mayers D F, 2005. Numerical solution of partial differential equations: an introduction. 2nd ed. Cambridge: Cambridge University Press.

Motamedi M, 1999. The survival and activity of bacteria in compacted bentonite clay in conditions relevant to high level radioactive (HLW) repositories. PhD thesis. Göteborg University, Sweden.

Motamedi M, Pedersen K, 1998. *Desulfovibrio aespoeensis* sp nov., a mesophilic sulfate-reducing bacterium from deep groundwater at Äspö hard rock laboratory, Sweden. International Journal of Systematic Bacteriology 48, 311–315.

Motamedi M, Karland O, Pedersen K, 1996. Survival of sulfate reducing bacteria at different water activities in compacted bentonite. FEMS Microbiology Letters 141, 83–87.

Muurinen A, Lehikoinen J, 1999. Porewater chemistry in compacted bentonite. Posiva 99-20, Posiva Oy, Finland.

Pedersen K, 2010. Analysis of copper corrosion in compacted bentonite clay as a function of clay density and growth conditions for sulfate-reducing bacteria. Journal of Applied Microbiology 108, 1094–1104.

Pedersen K, 2012a. Influence of H_2 and O_2 on sulphate-reducing activity of a subterranean community and the coupled response in redox potential. FEMS Microbiology Ecology 82, 653–665.

Pedersen K, 2012b. Subterranean microbial populations metabolize hydrogen and acetate under in situ conditions in granitic groundwater at 450 m depth in the Äspö Hard Rock Laboratory, Sweden. FEMS Microbiology Ecology 81, 217–229.

Pedersen K, Ekendahl S, 1990. Distribution and activity of bacteria in deep granitic groundwaters of southeastern Sweden. Microbial Ecology 20, 37–52.

Pedersen K, Motamedi M, Karnland O, Sandén T, 2000a. Cultivability of microorganisms introduced into a compacted bentonite clay buffer under high-level radioactive waste repository conditions. Engineering Geology 58, 149–161.

Pedersen K, Motamedi M, Karnland O, Sandén T, 2000b. Mixing and sulphate-reducing activity of bacteria in swelling, compacted bentonite clay under high-level radioactive waste repository conditions. Journal of Applied Microbiology 89, 1038–1047.

Pedersen K, Arlinger J, Eriksson S, Hallbeck A, Hallbeck L, Johansson J, 2008. Numbers, biomass and cultivable diversity of microbial populations relate to depth and borehole-specific conditions in groundwater from depths of 4–450 m in Olkiluoto, Finland. The ISME Journal 2, 760–775.

Pedersen K, Bengtsson A F, Edlund J S, Eriksson L C, 2014a. Sulphate-controlled diversity of subterranean microbial communities over depth in deep groundwater with opposing gradients of sulphate and methane. Geomicrobiology Journal 31, 617–631.

Pedersen K, Bengtsson A, Edlund J, Rabe L, Hazen T, Chakraborty R, Goodwin L, Shapiro N, 2014b. Complete genome sequence of the subsurface, mesophilic sulfate-reducing bacterium *Desulfovibrio aespoeensi*s Aspo-2. Genome Announcements 2, e00509-00514. doi:10.1128/genomeA.00509-14

Persson J, Lydmark S, Edlund J, Pääjärvi A, Pedersen K, 2011. Microbial incidence on copper and titanium embedded in compacted bentonite clay. SKB R-11-22, Svensk Kärnbränslehantering AB.

Potts M, 1994. Desiccation tolerance of prokaryotes. Microbiological Reviews 58, 755–805.

Rudnicki M D, Elderfield H, Spiro B, 2001. Fractionation of sulfur isotopes during bacterial sulfate reduction in deep ocean sediments at elevated temperatures. Geochimica et Cosmochimica Acta 65, 777–789.

Sandén T, Olsson S, Andersson L, Dueck A, Jensen V, Hansen E, Johnsson A, 2014. Investigation of backfill candidate materials. SKB R-13-08, Svensk Kärnbränslehantering AB.

SKB, 2010. Design and production of the KBS-3 repository. SKB TR-10-12, Svensk Kärnbränslehantering AB.

Stackebrandt E, 2014. The emended family *Peptococcaceae* and description of the families *Desulfitobacteriaceae*, *Desulfotomaculaceae*, and *Thermincolaceae*. In Rosenberg E, DeLong E F, Lory S, Stackebrandt E, Thompson F (eds). The prokaryotes: firmicutes and tenericutes. Berlin, Heidelberg: Springer, 285–289.

Stackebrandt E, Schumann P, Schuler E, Hippe H, 2003. Reclassification of *Desulfotomaculum auripigmentum* as *Desulfosporosinus auripigmenti* corrig., comb. nov. International Journal of Systematic and Evolutionary Microbiology 53, 1439–1443.

Stroes-Gascoyne S, Haveman S A, Hamon C J, Delaney T, Pedersen K, Arlinger J, Ekendahl S, Hallbeck L, Jahromi N, Dekeyser K, Daumas S, 1997. Occurrence and identification of micro-organisms in compacted clay-based buffer material designed for use in a nuclear fuel waste disposal vault. Canadian Journal of Microbiology 43, 1133–1146.

Svensson D, Dueck A, Nilsson U, Olsson S, Sandén T, Lydmark S, Jägerwall S, Pedersen K, Hansen S, 2011. Alternative buffer material. Status of the ongoing laboratory investigation of reference materials and test package 1. SKB TR-11-06, Svensk Kärnbränslehantering AB.

Widdel F, Bak F, 1992. Gram-negative, mesophilic sulphate-reducing bacteria. In Balows A, Trüper H G, Dworkin M, Harder W, Schleifer K-H (eds). The prokaryotes : a handbook on the biology of bacteria : ecophysiology, isolation, identification, applications. 2nd ed. New York: Springer, 3352–3378.

Pressures

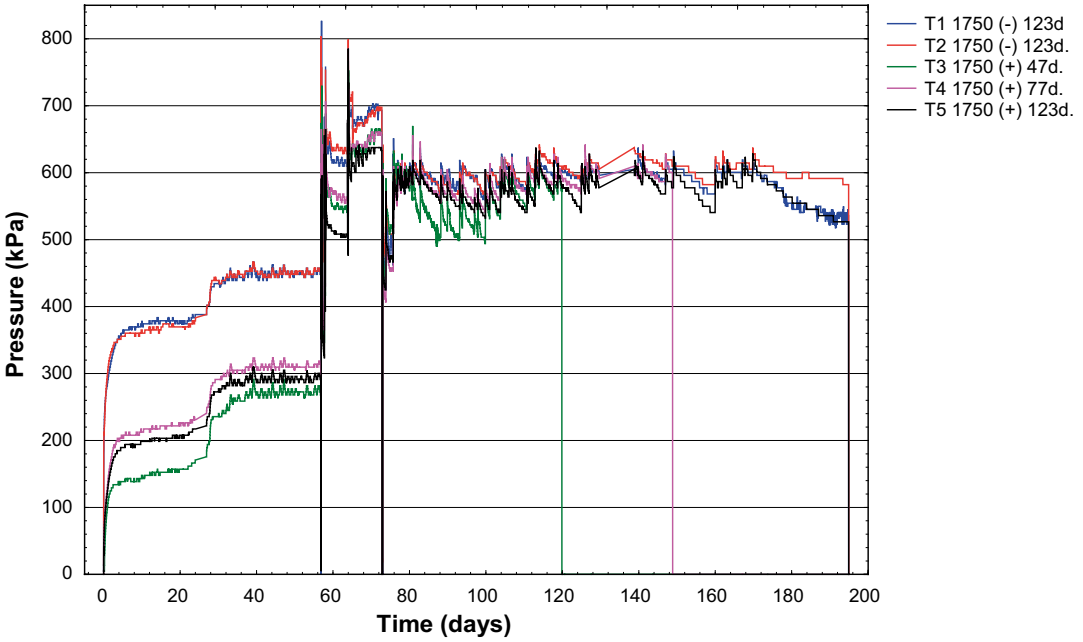

Figure A-1. *Pressures registered by force transducers for MX-80, experiment 1, 1 750 kg m^{-3} test cells according to symbol description.*

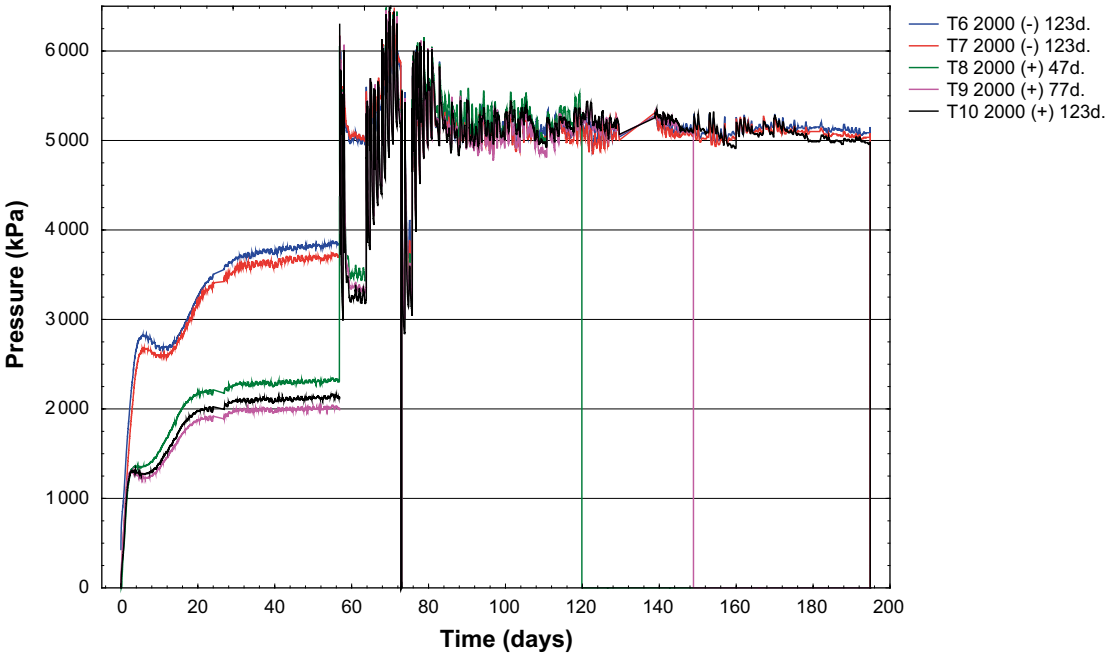

Figure A-2. *Pressures registered by force transducers for MX-80, experiment 1, 2 000 kg m^{-3} test cells according to symbol description.*

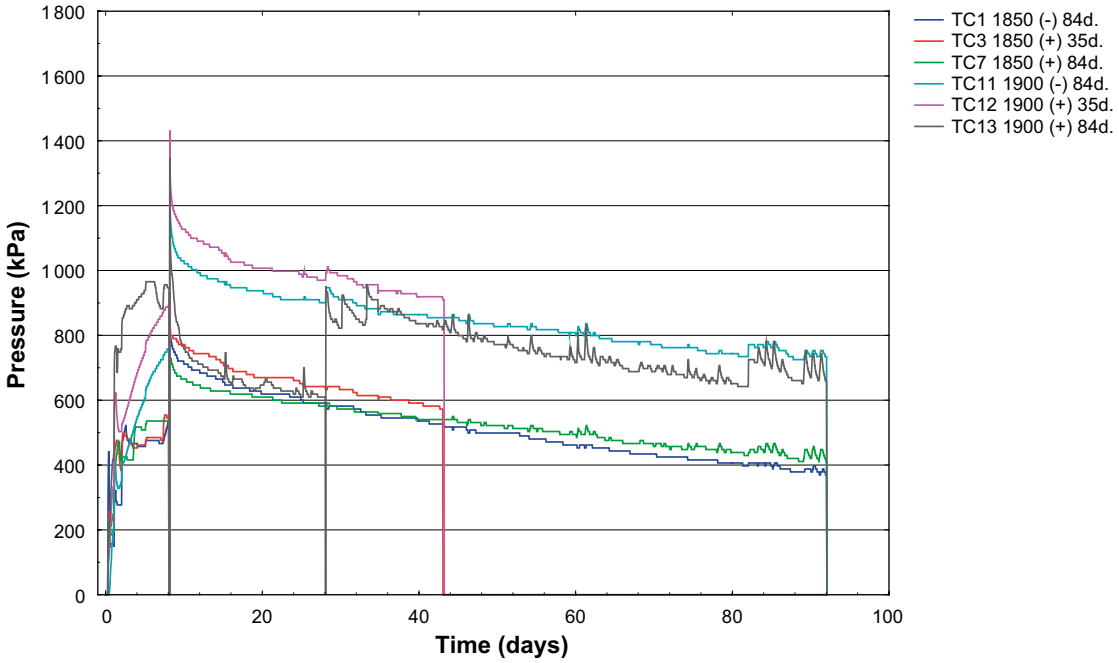

Figure A-3. *Pressures registered by force transducers for Asha and MX-80, experiment 2, 1 850 and 1 900 kg m^{-3} test cells according to symbol description.*

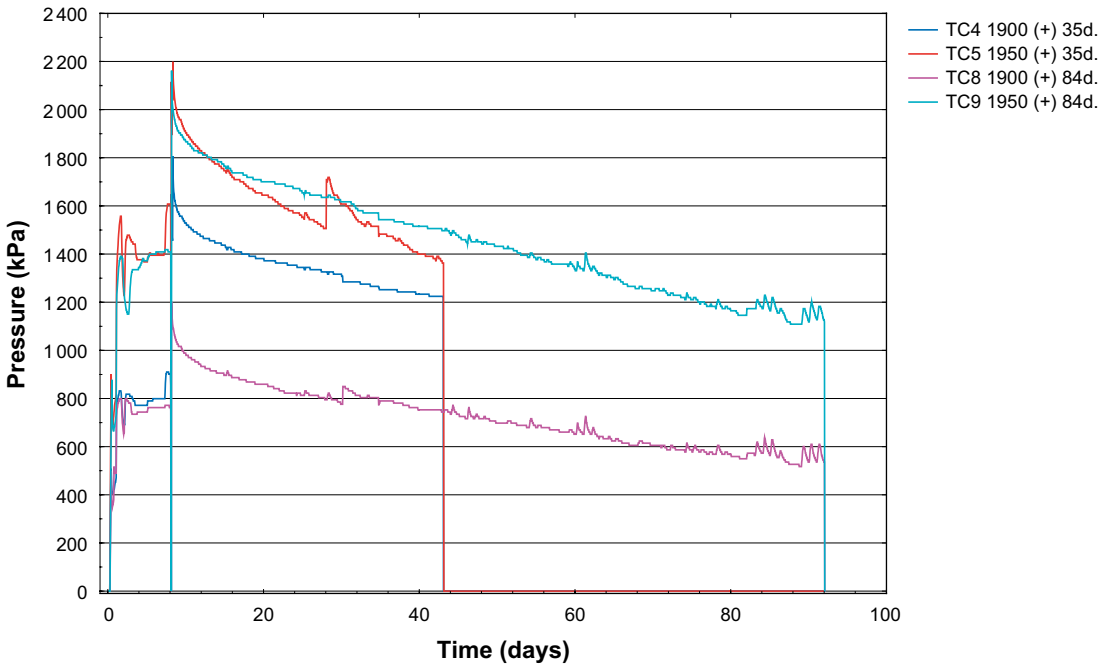

Figure A-4. *Pressures registered by force transducers for Asha, experiment 2, 1 900 and 1 950 kg m^{-3} test cells according to symbol description*

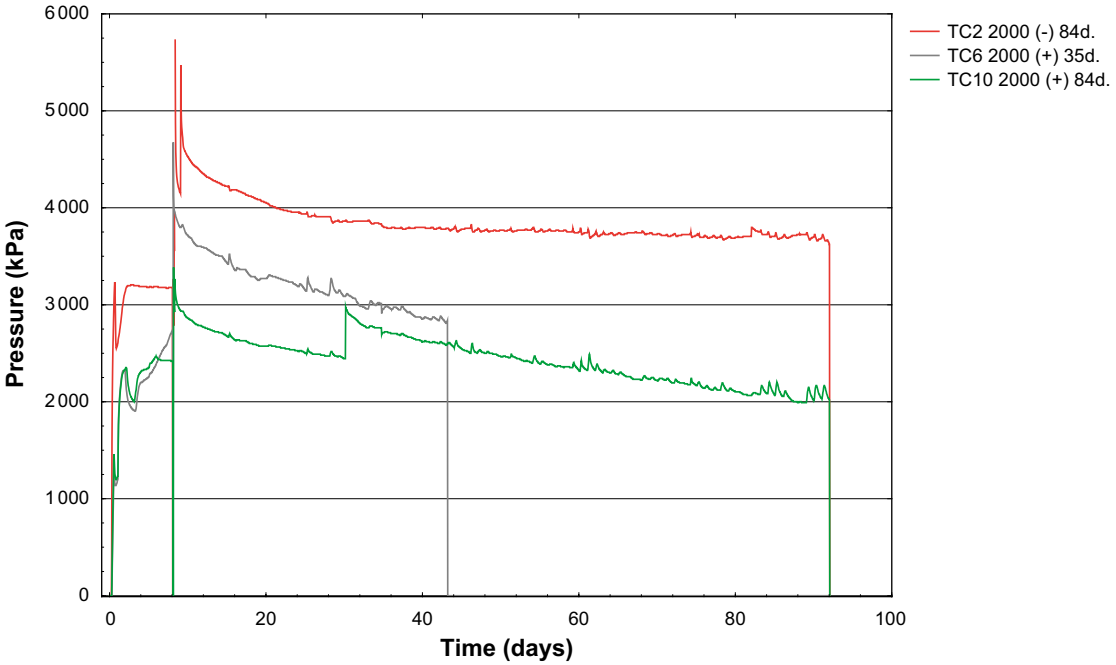

Figure A-5. *Pressures registered by force transducers for Asha, experiment 2, 2 000 kg m^{-3} test cells according to symbol description.*

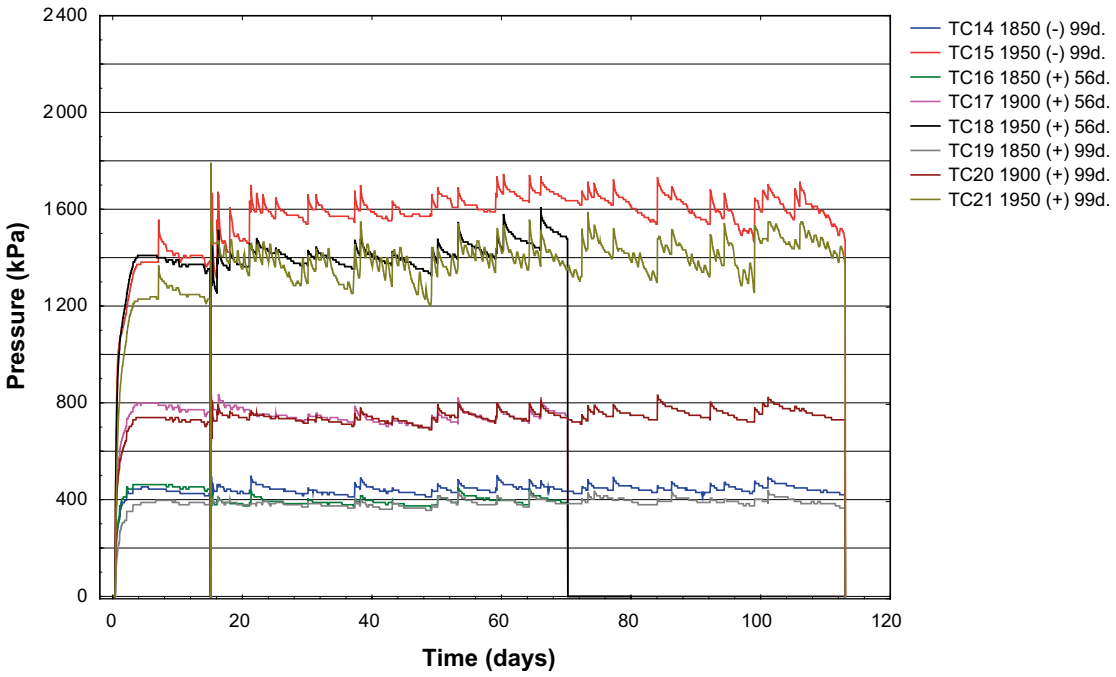

Figure A-6. *Pressures registered by force transducers for Calcigel, experiment 3, 1 850 to 1 950 kg m^{-3} test cells according to symbol description.*

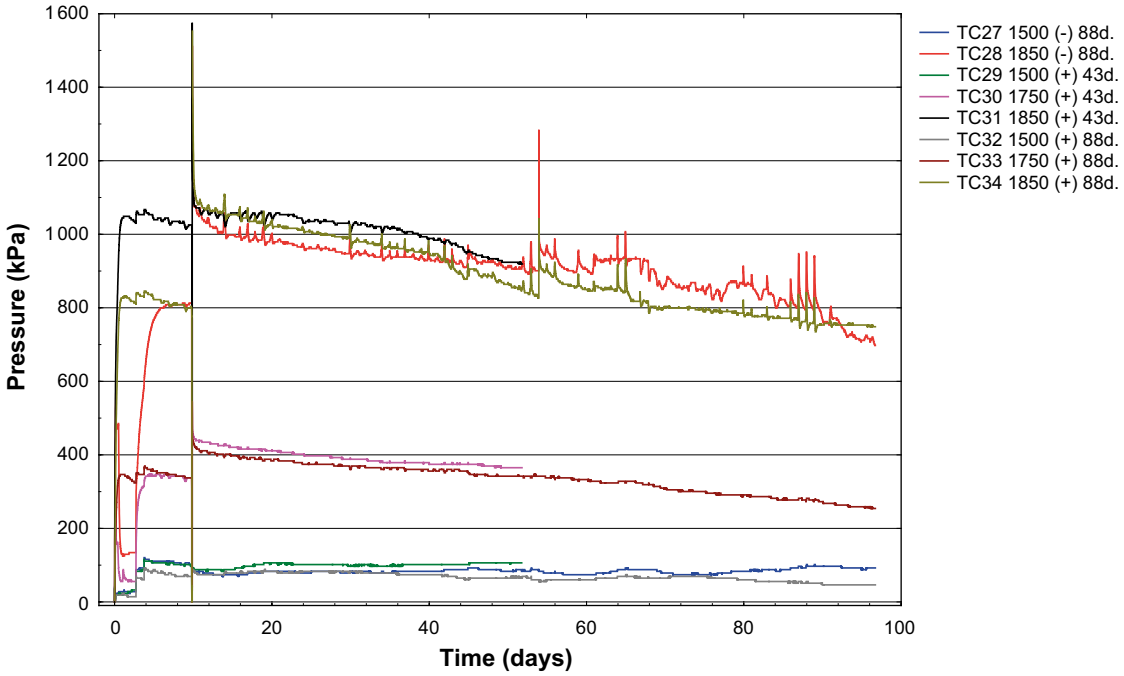

Figure A-7. *Pressure sregistered by force transducers for Asha, experiment 4, 1 500 to 1 850 kg m^{-3} test cells according to symbol description.*

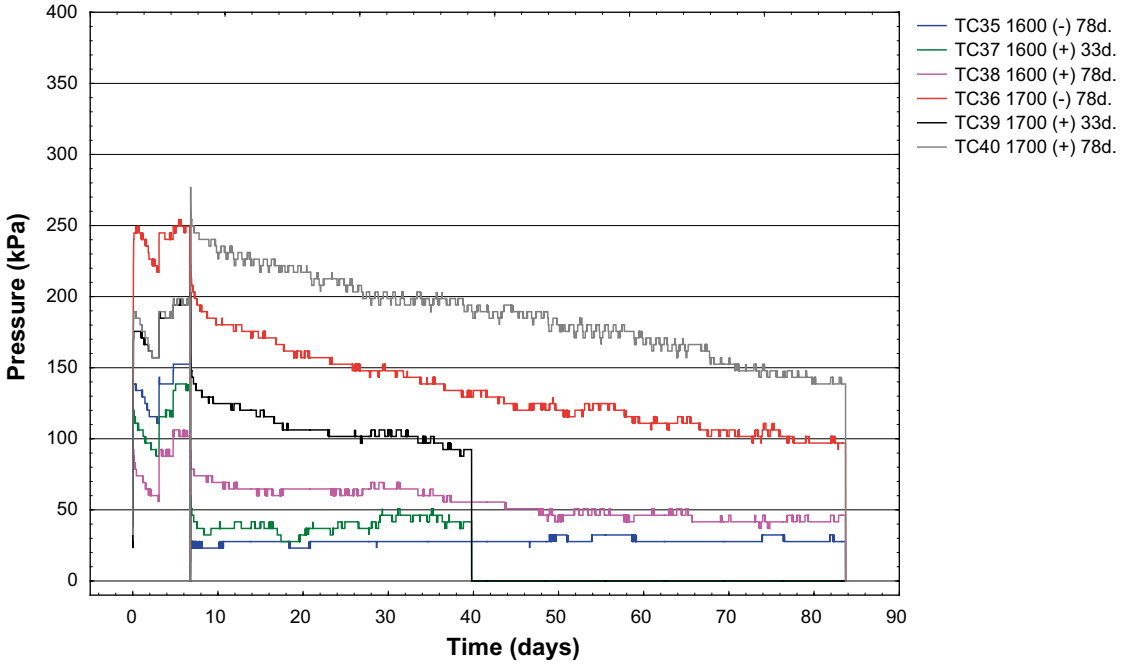

Figure A-8. *Pressuresregistered by force transducers for Asha, experiment 5, 1 600 to 1 700 kg m^{-3} test cells according to symbol description.*

Arkitektkopia AB, Bromma, 2017

SKB is tasked with managing Swedish nuclear and radioactive waste in a safe way.

skb.se